




Cite this: DOI: 10.1039/d0ee02981e

## Recent advances in innovative strategies for the CO<sub>2</sub> electroreduction reaction

Xinyi Tan,<sup>a</sup> Chang Yu,<sup>\*a</sup> Yongwen Ren,<sup>a</sup> Song Cui,<sup>a</sup> Wenbin Li<sup>a</sup> and  
Jieshan Qiu <sup>\*ab</sup>

The carbon dioxide electroreduction reaction (CO<sub>2</sub>RR), an emerging electrocatalysis reaction, is promising for converting CO<sub>2</sub> into value-added fuels or chemicals (e.g., hydrocarbons and oxygenates). However, the CO<sub>2</sub>RR system for practical evaluations and applications is still limited by its low current density and poor CO<sub>2</sub> utilization and conversion as well as dismal energy efficiency. To reach up to the practical application level, the components of the CO<sub>2</sub>RR device/system need to be systematically considered and optimized. This review specifically focuses on the latest and innovative design strategies toward each part of the system. In particular, the innovative and idiographic design strategies for tandem catalysts, promising electrolytes, upgraded electrodes, and advanced devices as well as anodic reactions are discussed at length. Moreover, some individual perspectives on opportunities and future challenges for each component of the CO<sub>2</sub>RR system are also provided. Perspectives and new trends presented in this review are not just labels and classifications. Instead, it is particularly expected that innovative ideas and visionary discussions in this review can systematically instruct and inspire researchers to contribute more efforts toward comprehensively optimizing the performance of the CO<sub>2</sub>RR system to a higher level.

Received 16th September 2020,  
Accepted 14th December 2020

DOI: 10.1039/d0ee02981e

rsc.li/ees

### Broader context

Global warming caused by excessive CO<sub>2</sub> emissions has drawn great attention of the world. The electroreduction technology is one of the promising ways to convert CO<sub>2</sub> into fuels and value-added fine chemicals by utilizing the intermittent electrical energy, finally achieving the artificial carbon loop. Nevertheless, the performance of this reaction system still faces serious challenges for the requirement of industrialization to some degree, such as the selectivity for C<sub>2</sub> and C<sub>2+</sub> products, low current density and poor CO<sub>2</sub> utilization and conversion, and dismal energy efficiency. To realize the large-scale industrialization of this reaction system, the components of CO<sub>2</sub>RR device/system are urgent to be systematically considered and optimized. Here, the latest and innovative design strategies for CO<sub>2</sub>RR system are systematically summarized and underlined for inspiring researchers to further develop and explore, including catalyst, electrolyte, electrode, device as well as anodic reaction. Above all, this review presents the new trends, visionary discussion, opportunities and future challenges, which can guide researchers to further comprehensively optimize the CO<sub>2</sub>RR device/system and overcome the key barriers, and finally upgrade it from laboratory level to industrial-scale in future.

## 1. Introduction

With the increasing amount of CO<sub>2</sub> accumulated in the atmosphere, the ensuing climatic and environmental crisis has serious implications, such as global warming and ocean acidification, and significantly challenges the sustainable development of

human society. The CO<sub>2</sub> electroreduction reaction (CO<sub>2</sub>RR) driven by renewable electricity is an emerging and promising technology for converting CO<sub>2</sub> into valuable fuels and fine chemicals in terms of its promoting sustainable chemistry and carbon neutrality.<sup>1,2</sup> However, the CO<sub>2</sub>RR system still faces various issues and tough challenges at present, such as its low current density and poor selectivity for C<sub>2</sub> or C<sub>2+</sub> products, mediocre stability, ultra-low CO<sub>2</sub> conversion, and dismal energy efficiency, which remarkably limit its practical implementations in the future.<sup>3–7</sup> Furthermore, it is also not sufficient to address these serious challenges merely by developing electrocatalysts further. Instead, to achieve the practical application level, the components of the CO<sub>2</sub>RR device/system need to be systematically considered<sup>8</sup> and are summarized

<sup>a</sup> State Key Lab of Fine Chemicals, School of Chemical Engineering, Liaoning Key Lab for Energy Materials and Chemical Engineering, Dalian University of Technology, Dalian 116024, China. E-mail: chang.yu@dlut.edu.cn, jqiu@dlut.edu.cn

<sup>b</sup> College of Chemical Engineering, Beijing University of Chemical Technology, Beijing 100029, China. E-mail: qiujs@mail.buct.edu.cn

in detail and shown in Fig. 1. The corresponding goals are related to the following aspects: (i) the key electrocatalyst in the cathode for achieving selective catalytic CO<sub>2</sub> conversion to value-added C<sub>2</sub> or C<sub>2+</sub> products; (ii) rational electrode structures with a stable three-phase reaction interface and fast mass transport, endowing the electrocatalyst with highly exposed active sites, finally helping to realize the required industrial-grade current density; (iii) the electrolyte for maintaining the microenvironment (including pH, and absorbed anionic and cationic species) of CO<sub>2</sub>RR and for weakening HER to enhance the selectivity toward the target products; (iv) a device with a low cell resistance, good stability, and simple assembly for obtaining a high CO<sub>2</sub> conversion rate and high yield of cathodic products; (v) the valuable anodic reaction with a low onset potential for achieving a high energy-efficient overall reaction process.

Although enormous efforts have been devoted to developing highly selective electrocatalysts for the CO<sub>2</sub>RR in the past several years, most excellent catalysts with industrial-grade current densities can only selectively convert CO<sub>2</sub> to CO at present.<sup>9–12</sup> While the production of value-added C<sub>2</sub> and C<sub>2+</sub> products mainly depend on Cu-based catalysts at present, the production suffers from poor selectivity and a high overpotential.<sup>13–19</sup> Therefore, highly selective catalyst systems capable of producing C<sub>2</sub> and C<sub>2+</sub> products still need to be developed and explored. In addition, most of the current electrodes are prepared by loading the powder catalyst on conductive substrates with the help of a binder, thus the active sites are not adequately exposed, and the three-phase interface on the electrode tends to be unstable, leading to limited gas diffusion and electron transfer.<sup>20,21</sup> In this respect, the electrode structures urgently need to be finely elaborated for eliminating the limitations of the current powder electrode. As for the electrolyte, there are still some major challenges for the CO<sub>2</sub>RR in the available electrolytes at present, such as strong competition with the HER, the difficulty of separating the

liquid products from the electrolyte solution,<sup>22</sup> CO<sub>2</sub> reacting with the alkaline electrolyte solution, and the low CO<sub>2</sub> solubility (0.034 M).<sup>23</sup> Although the traditional H cell may be convenient for CO<sub>2</sub>RR tests, it is hard to achieve an industrial current density due to the limited mass transport. Recently, some progress has been made in CO<sub>2</sub>RR devices, especially in the field of flow cells, which can enable CO<sub>2</sub>RR with appreciable current density (>200 mA cm<sup>-2</sup>).<sup>9</sup> However, more complex engineering designs for the device are required to realize the fast gas mass transport, electron transfer, high operation stability and CO<sub>2</sub> conversion efficiency for meeting the practical requirements and for evaluation.<sup>24,25</sup> Last but not the least, the effects of the anodic reaction should also be paid more attention to for the CO<sub>2</sub>RR system.<sup>26,27</sup> Generally, in conventional electrolytes, the anode reaction is a low-value oxygen evolution reaction (OER), but the energy consumption of OER can account for 90% of the entire system, due to its highly theoretical onset potential (1.23 V),<sup>28</sup> which seriously constraints achieving a high energy efficiency for the entire system. In view of this, there is an urgent demand for an alternative anode reaction to replace the conventional OER, one which could make the overall reaction more energy-efficient.<sup>26,29</sup>

Thus, to alleviate or address the above-mentioned issues, innovative and promising design strategies are highly required. In this review, we focus on the innovative and promising designing strategies for the CO<sub>2</sub>RR system recently proposed to tackle the issues and tough challenges involved with each component of the CO<sub>2</sub>RR system. The listed five parts that are addressed here are related to: the use of a tandem catalyst, promising electrolyte, upgraded electrode, advanced device, and hybrid CO<sub>2</sub> electrolysis, respectively, as schematically summarized in Fig. 2. To some extent, this places more challenges in rationally designing electrocatalysts toward C<sub>2</sub> and C<sub>2+</sub> products, using economic and beneficial electrolytes, constructing novel 3D free-standing electrodes, configuring the



**Chang Yu**

*Chang Yu received her PhD degree from the School of Chemical Engineering at Dalian University of Technology (DUT) in 2008. She is currently a full time professor at School of Chemical Engineering at DUT, and the winner of the Outstanding Youth Fellowship supported by the National Natural Science Foundation of China. Her research interests mainly focus on the preparation of value-added/functional carbon and their*

*coupled two-dimensional inorganic layered materials, and their application in supercapacitors, thermal/electrocatalytic conversion of small molecules and fine chemicals.*



**Jieshan Qiu**

*Jieshan Qiu received his PhD degree in organic chemical engineering in 1990 from Dalian University of Technology, China. Currently, he is Cheung-Kong Distinguished Professor of Carbon Science and Chemical Engineering, and the Dean of College of Chemical Engineering at Beijing University of Chemical Technology, China. Prof. Qiu is an internationally recognized researcher and thought leader in carbon science and chemical*

*engineering. His research encompasses both fundamental and applied aspects of carbon materials and science, with a focus on the methodologies for producing carbon materials and their applications in catalysis, energy storage and conversion.*

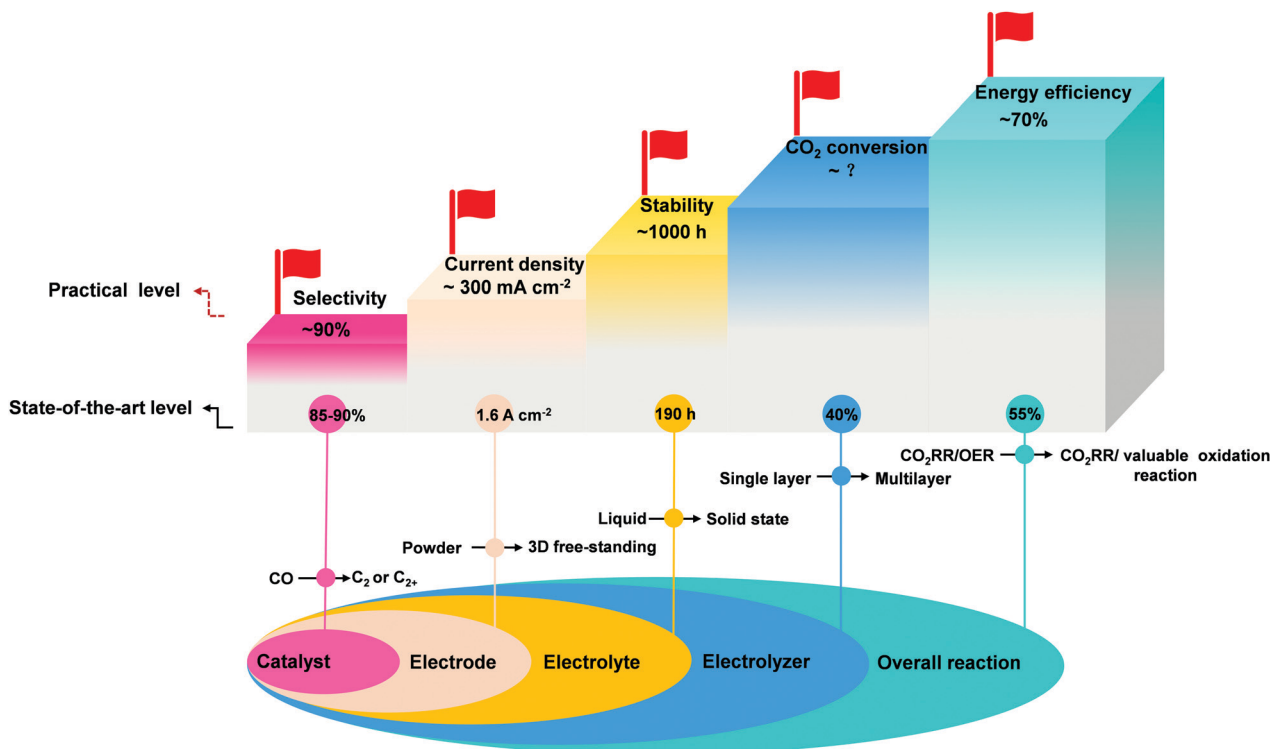


Fig. 1 Schematic illustration of the components involved in a CO<sub>2</sub>RR system and relevant challenges toward high-performance toward a practical level. State-of-the-art data of selectivity, stability, and energy efficiency for C<sub>2</sub> or C<sub>2+</sub> products on Cu nanoparticles, adopted from ref. 68. State-of-the-art data of current density, adopted from ref. 64. While state-of-the-art data of CO<sub>2</sub> conversion for CO production on Ag catalyst in multilayer electrolyzer, adopted from ref. 125. Requirements of CO<sub>2</sub>RR performance for practical level. Adapted with permission from ref. 6. Copyright 2019, Elsevier.

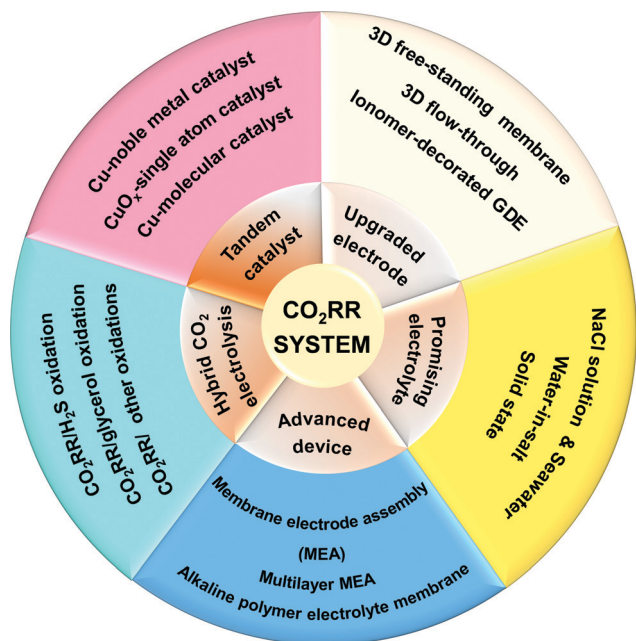


Fig. 2 Summarization of the innovative design strategies for CO<sub>2</sub>RR systems.

advanced devices without limited mass transport, and coupling the CO<sub>2</sub>RR with a valuable oxidation reaction for producing fine chemicals with high energy efficiency. The innovative and

unique ideas for addressing the critical issues of each part are summarized and presented, which should greatly inspire researchers to further explore these aspects. The novel ideas and discussion presented in this review should not be viewed separately, but should be systematically considered; finally instructing the design of CO<sub>2</sub>RR systems for comprehensively improving the selectivity for C<sub>2</sub> and C<sub>2+</sub> products, the current density, stability, energy efficiency, and CO<sub>2</sub> conversion efficiency to an impressive level for practical application in the future.

## 2. Innovative design strategies for the CO<sub>2</sub>RR

### 2.1. Tandem catalyst

In past several years, a large number of catalysts for CO<sub>2</sub>RR have been developed and exhibited comprehensive catalytic performance for CO production, such as molecular catalysts (porphyrin and phthalocyanine),<sup>30–39</sup> carbon-based single-atom catalysts,<sup>10,12,40–49</sup> and noble metal catalysts (Au, Ag, Pd),<sup>50–59</sup> which are partially shown in Fig. 3a and summarized in Table 1. In particular, it has been clearly found that the molecular, single-atom, and noble-metal catalysts can achieve a high faradaic efficiency (over 90%) and low overpotential for CO; while copper-based catalysts have attracted extensive attention by virtue of their unique capability for converting CO<sub>2</sub>

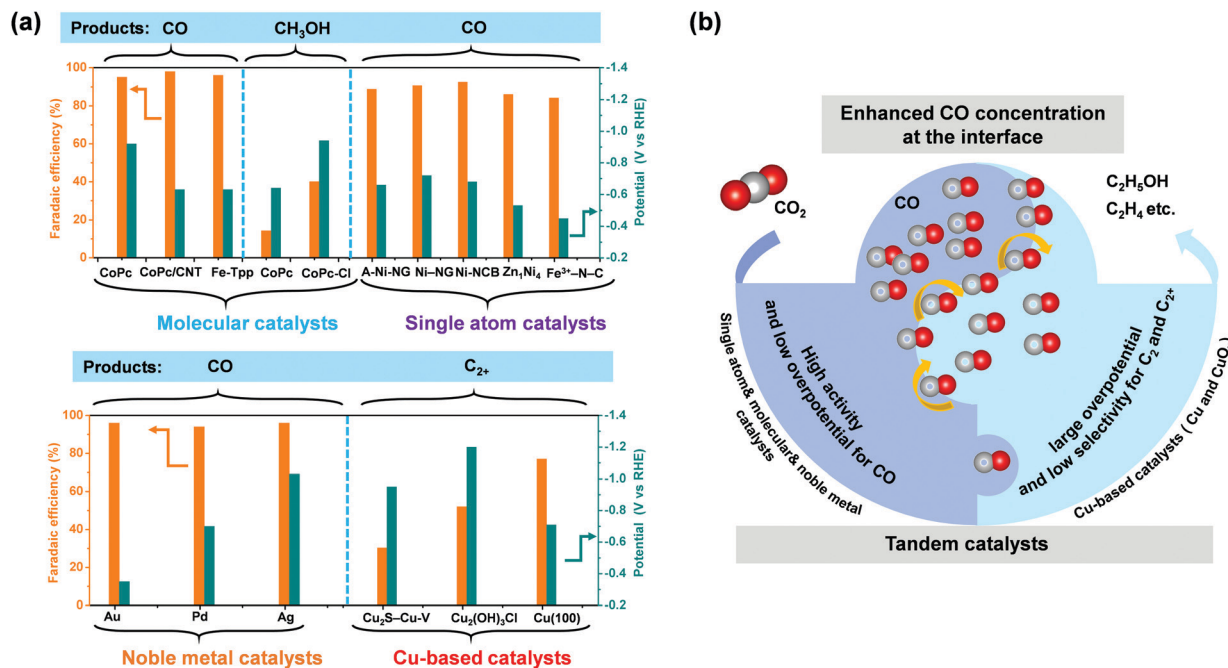


Fig. 3 (a) Comparison of FEs and applied potentials for various products over different catalysts during the CO<sub>2</sub>RR process. (b) Schematic of some smart arrangements for tandem catalysts with a synergistic catalysis reaction process.

molecules into various valuable products.<sup>16,60–68</sup> However, the Cu-based catalysts still face critical issues for producing C<sub>2</sub> and C<sub>2+</sub> products, such as a high overpotential and low selectivity, as shown in Fig. 3a, and some of these are partially summarized in Table 1. In this case, Cu species-containing tandem catalysts with high selectivity for C<sub>2</sub> and C<sub>2+</sub> products were proposed and have been gradually developed to address these issues, such as Cu–molecular catalysts, CuO<sub>x</sub>–single atom catalysts, and Cu–noble metal catalysts, and the available work now is schematically summarized in Fig. 3b. According to the mechanism of producing

C<sub>2</sub> and C<sub>2+</sub> products, it was noticed that CO is a key intermediate for achieving carbon–carbon (C–C) coupling and further for reduction to C<sub>2+</sub> products on the Cu-based catalysts.<sup>60,69–71</sup> Therefore, the barrier to CO production can be lowered on tandem catalysts, and in the meantime, the local concentration of CO on the surface of Cu-based catalysts can also be enhanced for achieving a high selectivity toward C<sub>2</sub> and C<sub>2+</sub> products. In view of this, as shown in Fig. 3b, with a smart arrangement among the above-mentioned catalysts, the synergistic effects of each part on tandem catalysts can be achieved, in which the

Table 1 Summary of the molecular, single atom, noble, Cu-based, and tandem catalysts for the CO<sub>2</sub>RR

Catalyst	Electrolyte	Product	Cathode potential vs. RHE (V)	FE (%)	<i>j</i> (mA cm <sup>-2</sup> )	Cell type	Ref.	
Molecular catalyst	CoPc/MWCNTS	1 M KOH	CO	-0.92	95	165	Flow cell	30
	CoPc/CNTS	0.1 M KHCO <sub>3</sub>	CO	-0.63	98	15	H cell	31
	Fe-PB	0.5 M KHCO <sub>3</sub>	CO	-0.63	96	~1.6	H cell	32
	CoPc-Cl	0.1 M KHCO <sub>3</sub>	CH <sub>3</sub> OH	-0.94	>40	>10	H cell	77
	CoPc/MWCNTS	0.1 M KOH	CH <sub>3</sub> OH	-0.64	14.3	0.68	H cell	78
Single atom catalyst	A-Ni-NG	0.5 M KHCO <sub>3</sub>	CO	-0.72	97	22	H Cell	40
	Ni-NG	0.5 M KHCO <sub>3</sub>	CO	-0.66	95	50	Flow cell	12
	Ni-NCB	0.5 M KHCO <sub>3</sub>	CO	-0.68	99	>100	Flow cell	41
	Zn <sub>1</sub> Ni <sub>4</sub>	1 M KHCO <sub>3</sub>	CO	-0.53	92	~14	H Cell	42
	Fe <sup>3+</sup> -N-C	0.5 M KHCO <sub>3</sub>	CO	-0.45	90	94	Flow cell	44
Noble metal catalyst	Au	0.5 M NaHCO <sub>3</sub>	CO	-0.35	96	2–4	H Cell	50
	Pd	0.5 M NaHCO <sub>3</sub>	CO	-0.90	92	40.2	H Cell	53
	Ag	0.1 M KHCO <sub>3</sub>	CO	-1.03	96	6	H Cell	52
Cu-based catalyst	CuS <sub>2</sub> -Cu-V	0.1 M KHCO <sub>3</sub>	C <sub>2</sub> and C <sub>2+</sub>	-0.95	~23	7.3	H Cell	60
	Cu <sub>2</sub> (OH)Cl	0.1 M KHCO <sub>3</sub>	C <sub>2</sub> and C <sub>2+</sub>	-1.20	52	31	H cell	61
	Cu (100)	7 M KOH	C <sub>2</sub> and C <sub>2+</sub>	-0.71	77	337	Flow cell	16
Tandem catalyst	FeTPP[Cl]-Cu	1 M KHCO <sub>3</sub>	C <sub>2</sub> and C <sub>2+</sub>	-0.82	~80	~242	Flow cell	73



molecular or single-atom catalysts or noble metal catalysts are responsible for producing CO and for boosting the local CO concentration on the surface of the Cu-based catalyst. Thus, it can be expected that the high CO<sub>2</sub>RR reactivity and selectivity for C<sub>2</sub> and C<sub>2+</sub> products can ultimately be realized on tandem catalysts.

Jaramillo *et al.* reported gold nanoparticles loaded on a polycrystalline copper foil (Au/Cu) and successfully applied this catalyst for the electrochemical transformation of CO<sub>2</sub> into liquid fuels.<sup>72</sup> The bimetallic Au/Cu tandem electrocatalyst displayed a cooperative activity and high selectivity superior to gold, copper, or AuCu alloys, with an increase of C<sub>2+</sub> products of over 100 times. Combining the electrochemical testing with gas transport modeling on the catalyst, it was indicated that the CO<sub>2</sub> reduction on the gold surface could enhance the local CO concentration on the nearby copper, where CO was further fast reduced to alcohols, such as ethanol and *n*-propanol, under local alkaline conditions. With the fast development of molecular catalysts for CO<sub>2</sub>RR, recently, a tandem catalyst consisting of a molecular catalyst and metal Cu (FeTPP[Cl]-Cu) was also developed,<sup>73</sup> and it achieved a faradaic efficiency (FE) of 41% for ethanol with a partial current density of 124 mA cm<sup>-2</sup>. Density functional theory (DFT) calculations, *in situ* Raman, and *operando* X-ray absorption spectra demonstrated that the FeTPP[Cl] molecular catalyst could have been responsible for producing CO, which was then converted to C<sub>2+</sub> products on a nearby Cu site, thus promoting carbon-carbon coupling and pushing the reaction pathway toward ethanol. In addition, a similar strategy has also been adopted to improve the CO<sub>2</sub>RR performance for C<sub>2</sub>H<sub>4</sub> production. For instance, Strasser *et al.* constructed a tandem catalyst made of a CuO<sub>x</sub> and NiNC single-atom catalyst (CuO<sub>x</sub>-NiNC),<sup>74</sup> which could achieve an increased C<sub>2</sub>H<sub>4</sub> yield up to 50%. Using *operando* differential electrochemical mass spectrometry and time-resolved isotope-labelling experiments, it was demonstrated that the enhanced C<sub>2</sub>H<sub>4</sub> production could be mainly attributed to a cross-coupling reaction pathway, and over two-thirds of the generated C<sub>2</sub>H<sub>4</sub> was from the conversion of co-fed CO gas. In this reaction system, the CuO<sub>x</sub> and NiNC single-atom catalyst served as active sites for the electrochemical catalysis of CO<sub>2</sub> to C<sub>2</sub>H<sub>4</sub> and CO, respectively, finally converting CO<sub>2</sub> into C<sub>2</sub>H<sub>4</sub> cooperatively. The discovery of the mechanism provides a theoretical basis for designing multi-component catalysts toward producing the target products in the future.

Moreover, carbon-based single-atom catalysts are also highly interesting for converting CO<sub>2</sub> into CO. Also as a non-metal-based catalyst, they possess many advantages, such as low cost, high conductivity, and specific surface area as well as adjustable pore structures.<sup>75,76</sup> In future, they may be used as promising and perfect supports for constructing tandem catalysts. With different target products, tandem catalysts based on single-atom catalysts need to be continuously developed, not only limited to tandem catalysts made of the single-atom and Cu-based catalyst above mentioned. According to recent work, the molecular catalysts can also produce value-added liquid products (Fig. 3a).<sup>77,78</sup> Thus, the more tandem catalysts are

possible, the greater the potential for boosting CO<sub>2</sub> conversion, selectivity, and the yield of CO<sub>2</sub>RR toward the target liquid or gas products, such as single-atom/molecule binary catalysts and single-atom/molecule/Cu-based ternary catalysts.

## 2.2. Upgraded electrode

In addition to the development of highly active catalysts, work on the architectures of the electrode has also made certain progress on improving the performance of CO<sub>2</sub>RR (Fig. 4), especially for facilitating gas mass transport and improving the current density. Generally, the as-prepared catalysts are powder materials. The electrode is usually prepared by loading powder catalysts on conductive substrates with the assistance of a binder (Fig. 4); however, this cannot meet the requirements for exposing the active sites as much as possible and for the fast mass transport and electron transfer at the reaction interface.<sup>20</sup> Therefore, there remains an urgent need to develop highly efficient electrodes with advanced architectures. Recently, 3D architecture electrodes, with tunable porous structures and highly exposed active sites, have exhibited extraordinary capabilities in mass transport and electron transfer, which make them extremely attractive for researchers to explore their applications in electrocatalysis reactions,<sup>79-81</sup> such as the OER and HER. Especially, in modularized flow-cell devices that will gain increasing popularity in practical applications, these 3D electrodes feature more obvious superiorities. In this respect, some emerging and upgraded electrodes that are used in the modularized flow-cell device have been reported and have displayed impressive performances for the CO<sub>2</sub>RR, such as the gas diffusion electrode (GDE), ionomer-decorated GDE, 3D flow-through electrode, 3D free-standing membrane electrode, and 3D N,P-co-doped carbon aerogels electrode.

The GDE, as a dominant structure of electrode, has exhibited outstanding performance and unique superiorities in the modularized flow-cell device.<sup>25,68,82-86</sup> A binder is commonly required to hold the powder electrocatalysts on the surface of the GDE (Fig. 4). The used binder, however, will cover a part of the active sites on the GDE, which is not expected. Moreover, the stability of the GDE also faces challenges in the flow-cell device due to the cathodic catalyst flooding and drop in the continuous flow of the electrolyte. Therefore, the structure of the GDE also needs to be further improved *via* a more meticulous design for obtaining a high current density and superior stability.

Sargent *et al.* developed a superfine ionomer-decorated GDE *via* integrating metal catalysts with porous 3D polytetrafluoroethylene (PTFE) as a substrate without using a binder.<sup>86</sup> Notably, the superfine ionomer layer with hydrophobic and hydrophilic functionalities played a significant role in the reaction interface, enabling the gas and ion transport together with electron transfer to set in together at the reaction interfaces. Simultaneously, the diffusion distance of the gas and ions on the electrode can be largely lengthened, leading to a highly enhanced availability of CO<sub>2</sub> on the electrode. In an alkaline electrolyte, this advanced electrode displayed the highest current density for ethylene so far, with a partial current density of 1.3 A cm<sup>-2</sup> and energy efficiency of 45%.

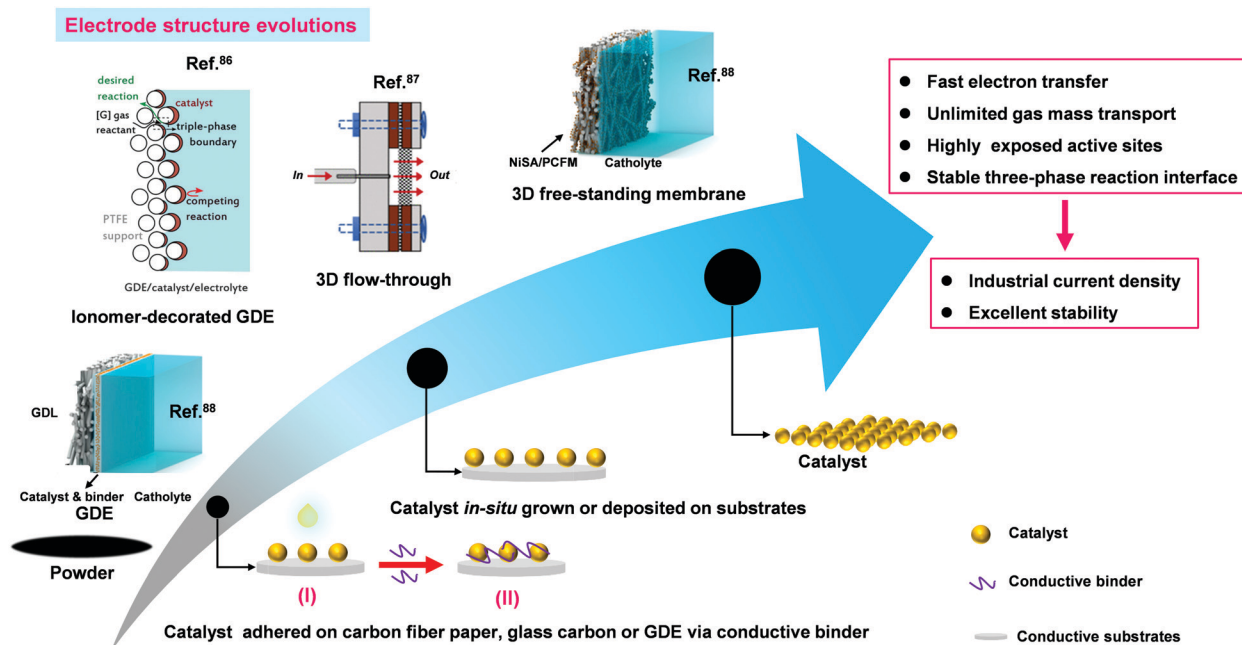


Fig. 4 Development of the electrode architecture from powders to 3D free-standing electrodes.

This superfine electrode engineering provides a novel idea for the further elaborate design and construction of a 3D electrode to promote the mass transport of the gas and to accelerate the reaction rate at the three-phase reaction interface.

Biener *et al.* constructed a 3D flow-through electrode by electrochemically depositing Ag nanoflowers on commercial macroporous Al foams (Fig. 4), in which the electrolyte and CO<sub>2</sub> continuously passed through it.<sup>87</sup> By using an ionic liquid electrolyte ([EMIM]BF<sub>4</sub>) as the electrolyte for its high solubility toward CO<sub>2</sub>, it could achieve a 70-fold increase toward the partial CO current density, and a 7-fold increase in FE toward CO. At the same time, the selectivity of the main product could be changed from oxalate to CO in the flow-through electrode configuration in comparison with the original. These results demonstrated that the flow-through electrode configuration is also one of the potential candidates for controlling the selectivity and overcoming the mass-transport limitations of the CO<sub>2</sub>RR.

In another case, a 3D membrane electrode without the substrates was also investigated and offered promise in flow-cell devices. He *et al.* constructed a 3D free-standing membrane electrode on the basis of an electrospinning technique,<sup>88</sup> which could be directly used as a GDE. The 3D free-standing membrane electrode could establish an extremely stable three-phase interface for CO<sub>2</sub>RR. Thus, it could achieve an industrial-grade current density (308.4 mA cm<sup>-2</sup>) with a CO FE of 88% under continuous operation for 120 h. This work opens the door for directly using free-standing electrodes as GDEs and will further guide the design and development of electrodes. Recently, Han *et al.* developed a 3D N,P-co-doped carbon aerogels (NPCA) catalyst, which could also be directly used as an electrode for the CO<sub>2</sub>RR.<sup>89</sup> Profiting from the high electrochemical surface area and good electrical conductivity,

the as-prepared 3D NPCA catalyst achieved a high CO FE of 99.1% with a record-breaking current density of 143.6 mA cm<sup>-2</sup> in an ionic liquid electrolyte.

### 2.3. Promising electrolytes

In addition to the catalysts, the electrolyte also plays a crucial role in electrochemical reactions due to its pH effects and ion effects. Also, it can drive the catalyst to restructure and produce the active species for the CO<sub>2</sub>RR through interacting with intermediates and products on the surface of the electrode.<sup>3,13,90–92</sup> It was demonstrated that the activities and selectivity varied with the use of different electrolytes in previous work.<sup>93–97</sup> In addition, the artificial electrolytes are consumable chemicals in the whole system, which has side effects on the economic and environmental benefits of CO<sub>2</sub>RR to some degree.<sup>98</sup> At present, the most commonly used artificial electrolytes are the inorganic electrolytes. Occasionally, some organic electrolytes are also applied for the CO<sub>2</sub>RR, such as [Bmim]PF<sub>6</sub> and EMIM-BF<sub>4</sub> (ionic liquids), methanol, and acetonitrile,<sup>89,97,99,100</sup> but they are expensive or low conductivity and thus limited in large-scale use. The inorganic electrolytes mainly include potassium hydroxide (KOH), sodium hydroxide (NaOH), potassium bicarbonate (KHCO<sub>3</sub>), and sodium bicarbonate (NaHCO<sub>3</sub>).<sup>95,96,101</sup> However, there are also some great challenges, especially with inorganic electrolytes, such as CO<sub>2</sub> reacting with the electrolyte in alkaline electrolytes and the strong side reaction of hydrogen evolution in nearly neutral electrolytes (Fig. 5a). Besides, the liquid products of the CO<sub>2</sub>RR in the cathode can be dissolved in the electrolyte and can further penetrate through the membrane in to the anode, which is not conducive to their precise detection and further separation and collection.<sup>102</sup> In response to some of the challenges for performing the CO<sub>2</sub>RR in different electrolytes,

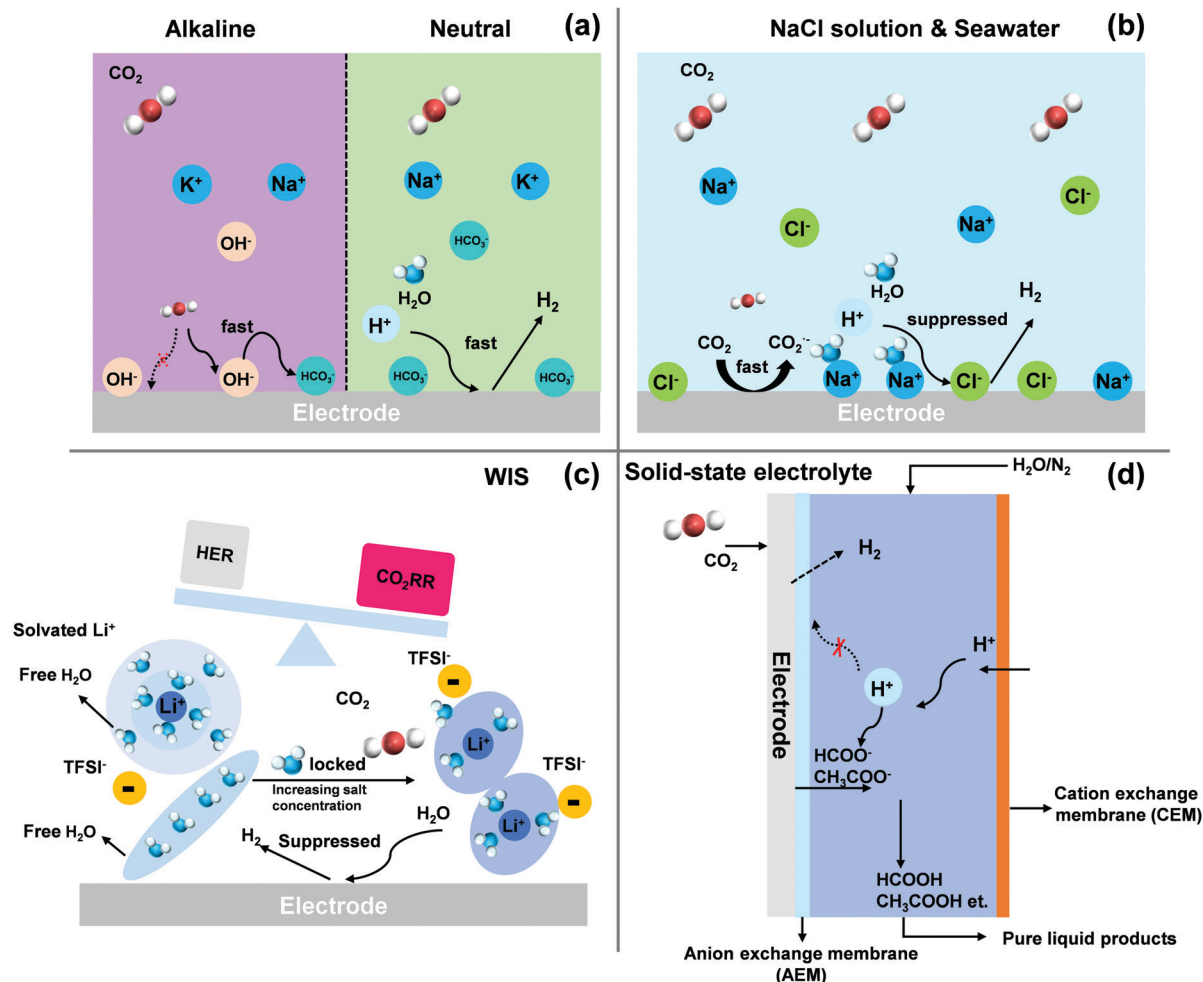


Fig. 5 Visual illustrations of the potential advantages and disadvantages in the CO<sub>2</sub>RR of various electrolyte systems on the surface of the electrode. (a) KOH/NaOH alkaline electrolyte and KHCO<sub>3</sub>/NaHCO<sub>3</sub> neutral electrolyte. (b) NaCl solution or seawater electrolyte. Adapted with permission from ref. 103. Copyright 2015, The Royal Society of Chemistry. (c) WIS electrolyte. (d) Solid-state electrolyte. Adapted with permission from ref. 119. Copyright 2019, Springer Nature.

some promising electrolyte systems, including NaCl solution and seawater, water-in-salt electrolytes, and solid-state electrolytes, have been adopted and developed for alleviating or solving these issues to some degree.

**NaCl solution and seawater.** NaCl solution as an electrolyte for the CO<sub>2</sub>RR actually exhibits some unique superiorities in comparison to the common electrolytes. Jia *et al.* employed NaCl solution as the electrolyte and achieved a CO FE of 93% over the as-prepared Zn catalyst.<sup>103</sup> Notably, the performance of the CO<sub>2</sub>RR in NaCl solution is superior to other conventional electrolytes. Moreover, the influence of anions (F<sup>-</sup>, Cl<sup>-</sup>, Br<sup>-</sup>, I<sup>-</sup>) on the CO<sub>2</sub>RR was also further investigated. As a result, the as-prepared Zn electrode also achieved the highest performance for CO<sub>2</sub>RR in NaCl solution. In this way, the superior performance of the Zn electrode was attributed to the effects of Cl<sup>-</sup> ions, where the Cl<sup>-</sup> ions suppressed the HER process, which facilitated the formation of CO<sub>2</sub><sup>•-</sup> intermediates (Fig. 5b). Similar effects of halogen ions in the electrolyte were also confirmed in previous work, especially for Cu catalysts, which could significantly improve the FE toward C<sub>2</sub> products.<sup>64,104–106</sup>

In addition, the author also found that the Fe single-atom catalyst also displayed a relatively prominent FE towards CO in NaCl solution in comparison with that in other conventional electrolytes.<sup>107</sup> Significantly, when the NaCl solution was used as the electrolyte, the OER in the anode was replaced by the chlorine evolution reaction (CER). In this way, for this device, the overall reaction comprised the CO<sub>2</sub>RR in the cathode and the CER in the anode, which allowed achieving a high energy efficiency, with the production of value-added products at both the cathode and anode.<sup>76,108</sup> This further demonstrated that the use of NaCl solution as the electrolyte has its potential advantages and merits. Besides, the Na<sup>+</sup> in the electrolyte also has an important effect on the selectivity of the C<sub>2+</sub> products formation.<sup>109</sup> Therefore, given the synergetic effects of Na<sup>+</sup> and Cl<sup>-</sup> ions, the use of NaCl solution as an electrolyte for the CO<sub>2</sub>RR should also be taken seriously and is worth further investigation.

In view of the superior performance in NaCl solution, there is no doubt that the abundant seawater on earth with good conductivity would be an ideal, economical, and promising electrolyte solution for the CO<sub>2</sub>RR. Einaga *et al.* used seawater

as the electrolyte for the CO<sub>2</sub>RR on boron-doped diamond electrodes.<sup>110</sup> The CO<sub>2</sub>RR could be successfully operated in seawater, which was indicative of a certain selectivity for formaldehyde. Wallace *et al.* also used seawater as an electrolyte, where appreciable performance for converting CO<sub>2</sub> to CO, with a high FE of 93 ± 3% could be achieved over an as-made Ag nanoparticle catalyst.<sup>111</sup> Meanwhile, it was also demonstrated that the Ca<sup>2+</sup> in seawater has a negative impact on the performance of the CO<sub>2</sub>RR. Recently, Luo *et al.* developed N-doping Ti<sub>3</sub>C<sub>2</sub> MXene nanosheets with titanium vacancies (VTi) *via* NH<sub>3</sub>-etching pyrolysis treatment.<sup>112</sup> In this work, it was confirmed that the N-doping Ti<sub>3</sub>C<sub>2</sub> MXene nanosheets displayed a remarkable 92% FE for CO and superior long-term stability over 40 h in seawater. The use of natural seawater as an electrolyte with other catalyst systems, such as porous carbon catalyst with abundant defects derived from pyrolyzing ZnO NP@ZIF-8, was also demonstrated,<sup>113</sup> achieving a high FE (over 90%) for CO, which further suggested the feasibility of the CO<sub>2</sub>RR being performed in natural seawater.

Notably, the use of seawater as a natural electrolyte has some inherent advantages, such as high CO<sub>2</sub> dissolution characteristics,<sup>114</sup> abundant halogen ions (Br<sup>-</sup>, I<sup>-</sup>, Cl<sup>-</sup>),<sup>115</sup> and good conductivity.<sup>116</sup> Therefore, the use of seawater as a natural and economical electrolyte is worthwhile for researchers to put more efforts into it for facilitating its practical application in the CO<sub>2</sub>RR. Correspondingly, catalysts that can be operated in seawater should also attract more attention and will need to be developed.

**Water-in-salt (WIS).** As is well known, the HER reaction is the only side reaction in the CO<sub>2</sub>RR in conventional electrolytes, which is difficult to inhibit due to its relatively low theoretical potential and fast reaction kinetics.<sup>19,23,117</sup> Recently, Wang *et al.* developed a unique WIS electrolyte system for the CO<sub>2</sub>RR process *via* using LiTFSI as a salt for inhibiting the undesired HER,<sup>118</sup> as depicted in Fig. 5c. In this system, the strong solvation effects in a high concentration of the salt electrolyte enabled the free H<sub>2</sub>O to be converted to solvated H<sub>2</sub>O, further locking down the free H<sub>2</sub>O molecules. Thus, the HER was greatly suppressed, leading to an enhanced CO FE from 30% in 0.5 M NaHCO<sub>3</sub> electrolyte of to up to 80% in WIS. More importantly, kinetic studies revealed that the reaction rate exhibited a pseudo-zeroth-order dependence on the water molecules, which suggested that the rate-determining step was electron transfer to the adsorbed CO<sub>2</sub> rather than proton transfer to CO<sub>2</sub><sup>•-</sup>. Moreover, in this novel electrolyte system, the side reactions of HER could be strongly inhibited. In general, the WIS electrolyte has obvious superiorities for inhibiting the competing HER on the CO<sub>2</sub>RR, and may widen the operating potential window for the CO<sub>2</sub>RR. Therefore, it is worth developing more WIS electrolyte systems for the CO<sub>2</sub>RR as well as for other electrocatalysis reactions, such as the nitrogen reduction reaction.

**Solid-state electrolytes.** When the target product is a liquid product, it is difficult to separate the product from the conventional liquid electrolytes. Meanwhile, certain amounts of liquid products may also penetrate the membrane to the anode, thus lowering the yield of liquid products. It is also much harder to

directly convert CO<sub>2</sub> to a pure liquid product *via* the CO<sub>2</sub>RR in conventional electrolytes. In view of this, Wang *et al.* constructed a solid-state electrolyte system, which consisted of ion-conducting polymers with different functional groups, to convert CO<sub>2</sub> into pure liquid products,<sup>119</sup> as given in Fig. 5d. The humid CO<sub>2</sub> was directly supplied to the cathode and the generated HCOO<sup>-</sup> reacted with protons generated from water oxidation to form pure HCOOH solution, and HER was also inhibited. In addition, pure HCOOH solution with a wide range of concentrations could be tuned by adjusting the flow rate of the deionized water in the cathode, up to a maximum value of 12 M. Furthermore, using a Cu catalyst, it was also demonstrated that this solid-state electrolyte system could be used for producing other C<sub>2+</sub> liquid oxygenates, including acetic acid, ethanol, and *n*-propanol. More importantly, the solid-state electrolyte system would open up a new way to produce pure liquid products *via* the CO<sub>2</sub>RR. Also, the development and use of various solid-state electrolytes that can be matched with suitable and selective catalysts would also be a new trend for producing value-added liquid products in the future.

#### 2.4. Advanced devices

Generally speaking, the CO<sub>2</sub>RR test is carried out in the traditional H cell device due to its easy accessibility and simple operation. Nevertheless, the gas mass transport in the whole process is inhibited to a great degree, leading to a limited current density and inhibiting its further practical application.<sup>5,120</sup> With the fast development of the CO<sub>2</sub>RR, it is also required that the performance of the CO<sub>2</sub>RR is evaluated regarding attaining a commercial-level current density and high conversion efficiency for finally moving the CO<sub>2</sub>RR from the laboratory to industrial application in the future.<sup>29</sup> In previous work, by using a flow-cell device with a stable three-phase reaction interface and unlimited gas mass transport and fast electron transfer on the electrode, the CO<sub>2</sub>RR could achieve a considerable current density and FE.<sup>82,84,121,122</sup> Therefore, much attention has been paid to device engineering for boosting and fully displaying the CO<sub>2</sub>RR performance, especially in flow-cell devices. In this context, we would emphasize that some novel and inspired devices have emerged for CO<sub>2</sub>RR recently, including the membrane electrode assembly (MEA) electrolyzer, the multilayer MEA electrolyzer (parallel or serial connection operation), and the alkaline polymer electrolyte membrane (APEM) electrolyzer, as shown in Fig. 6a–d.

At present, in order to obtain a high concentration of multi-carbon products and achieve a high CO<sub>2</sub> conversion efficiency as well as improved operating stability for the CO<sub>2</sub>RR, Sargent *et al.* presented an MEA electrolyzer (Fig. 6a), in which humidified CO<sub>2</sub> was directly used as a feedstock without a cathodic electrolyte.<sup>123</sup> Besides, cathodic and anodic catalysts were pressed together with the anion exchange membrane. In this way, the resistance of the device was greatly reduced, thus improving the current density for the CO<sub>2</sub>RR. Notably, in this MEA device, the CO<sub>2</sub>RR could be stably operated at a constant current density (150 mA cm<sup>-2</sup>) with a lower voltage and for over 2 h operating time or 120 mA cm<sup>-2</sup> for 100 h, which was



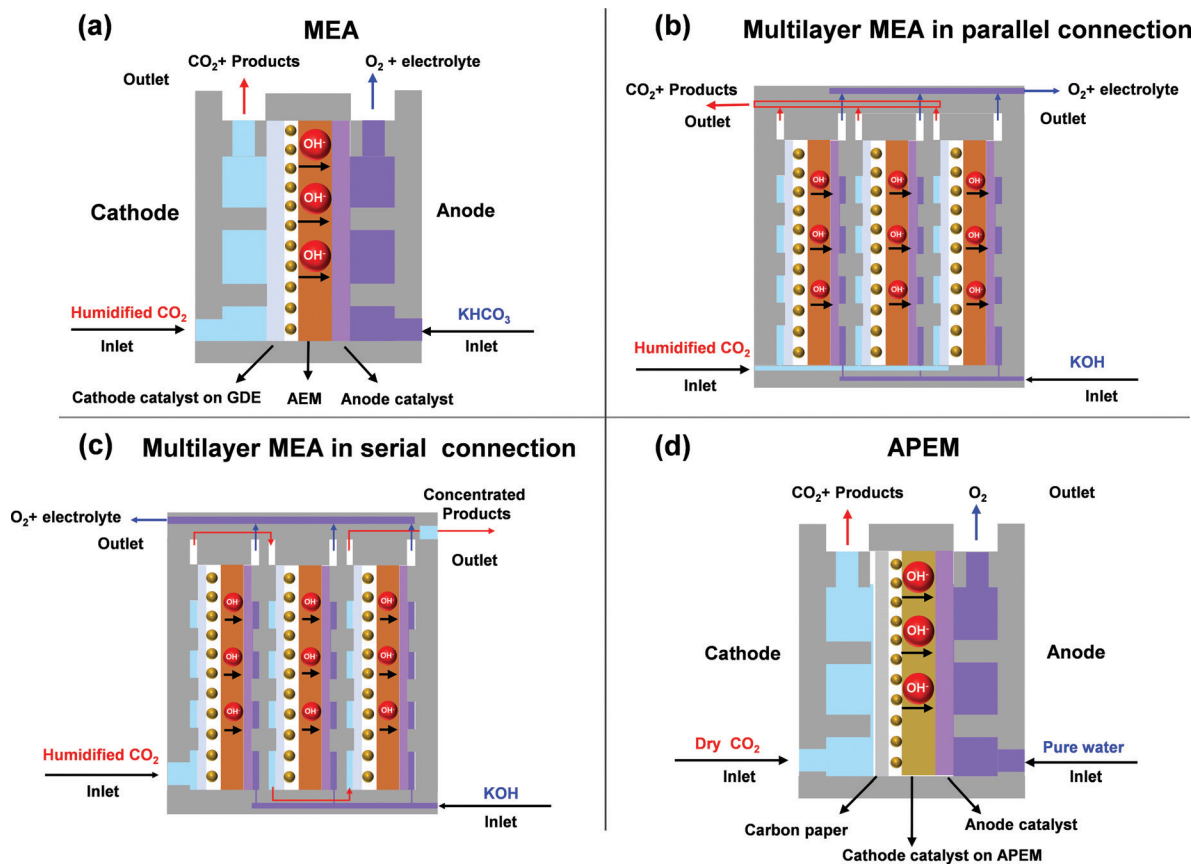


Fig. 6 Schematic of advanced devices for the CO<sub>2</sub>RR. (a) MEA electrolyzer separated by an anion exchange membrane (AEM), in which humidified CO<sub>2</sub> was supplied to the cathode and the KHCO<sub>3</sub> electrolyte circulated in the anode. Adapted with permission from ref. 123. Copyright 2019, Elsevier. (b and c) Multilayer MEA device for the CO<sub>2</sub>RR in parallel connection and serial connection on the basis of the MEA unit, respectively. (b and c) Adapted with permission from ref. 125. Copyright 2019, American Chemical Society. (d) APEM device, which can be operated with dry CO<sub>2</sub> in the cathode and pure water as the feedstock in the anode. Adapted with permission from ref. 126. Copyright 2019, The Royal Society of Chemistry.

superior to that achieved in previous alkaline and neutral flow-cells. This device could achieve 50% and 80% FEs for ethylene and C<sub>2+</sub> products, respectively, with a high outlet concentration of up to 30% ethylene and 4 wt% ethanol.

Considering the utilization of CO<sub>2</sub>, its conversion efficiency is really low in most of the reported works (<10%).<sup>124</sup> To improve the yield of the target products for the CO<sub>2</sub>RR and the CO<sub>2</sub> conversion efficiency, Janaky *et al.* first reported a multilayer electrolyzer for the CO<sub>2</sub>RR *via* a parallel or serial connection on the basis of an MEA unit,<sup>125</sup> respectively, as shown in Fig. 6b and c. When the cells were connected in parallel, the electrochemically active surface area was increased and the device achieved a similar partial current density as a single-cell electrolyzer. In particular, when the cells were connected in series, at low cell voltage (2.75 V), it displayed a high CO<sub>2</sub> conversion efficiency (up to 40%), and a high FE (95%) for CO production with partial current densities of above 250 mA cm<sup>-2</sup>. This was also a breakthrough for scaling up the CO<sub>2</sub>RR technique to practical levels. More importantly, the multilayer MEA electrolyzer with a smart design will inevitably inspire some researchers to concentrate on the conversion efficiency of CO<sub>2</sub> instead of only trying to achieve a high FE.

Moreover, Zhuang *et al.* constructed an APEM electrolyzer integrating the electrolyte, membrane, and catalyst in an all-in-one.<sup>126</sup> This strategy made the CO<sub>2</sub>RR electrolyzer operate with pure water, in which dry CO<sub>2</sub> could serve as the feedstock (Fig. 6d). In this device, an alkaline polymer electrolyte and quaternary ammonia poly(*N*-methyl-piperidine-*co-p*-terphenyl) (QAPPT) with high ionic conductivity and good mechanical properties were used as the membrane separator and the ionomer, and were impregnated into the electrodes. Using Au as a catalyst in the cathode, the FE for CO was over 85%, and the OER occurred at the IrO<sub>2</sub> anode fed with pure water. At 2.25 V, 50 °C, the stability of this electrolyzer could be maintained for over 100 h with no decay in the CO FE (90–95%). The construction strategy of this electrolyzer enabled the current density of the CO<sub>2</sub>RR to reach the level of industrialization and thus shows great prospects for practical application. Moreover, the electrolyzer was simply assembled and possessed a membrane electrode structure, which could be further extended for producing multi-carbon or value-added liquid products, and even to other electrocatalysis reactions.

In the above, several advanced devices with innovative designs have been presented and their advantages and

Table 2 Summary of the key components, operating conditions, and corresponding parameters in the performance of advanced CO<sub>2</sub>RR devices

Device type	Key component					Product	Cell voltage (V)	FE (%)	<i>j</i> (mA cm <sup>-2</sup> )	Stability (h)	<i>T</i> (°C)	Ref.
	Membrane	Catalyst		Electrolyte								
		Cathode	Anode	Cathode	Anode							
MEA	AEM <sup>c</sup>	Cu	IrO <sub>2</sub>	—	0.1 M KHCO <sub>3</sub>	C <sub>2</sub> H <sub>4</sub>	3.75	>40	120	100	40	123
Multilayer MEA	AEM <sup>c</sup>	Ag	Ir	—	1 M KOH	CO	2.75	85	~125	—	22 ± 2	125 <sup>a</sup>
	AEM <sup>c</sup>	Ag	Ir	—	1 M KOH	CO	2.75	95	250	8	60	125 <sup>b</sup>
APEM	APM <sup>d</sup>	Au/C	IrO <sub>2</sub>	APE <sup>e</sup>	Pure H <sub>2</sub> O	CO	2.25	90–95	100	>100	60	126

<sup>a</sup> Operation in parallel connection conditions. <sup>b</sup> Operation in serial connection conditions. <sup>c</sup> AEM, anion exchange membrane. <sup>d</sup> APM, alkaline polymer membrane. <sup>e</sup> APE, alkaline polymer electrolyte.

functions discussed. For convenient comparison, the key components, operating conditions, and corresponding parameters of these devices are summarized in Table 2 in detail. The MEA electrolyzer could achieve an industrial-scale current density with superior stability, due to its low cell resistance and fast mass transfer. The multilayer MEA electrolyzer was actually constructed by connecting multiple MEA units in serial or parallel, thus being able to further boost the CO<sub>2</sub> conversion and yield of the corresponding product. As for APEM, dry CO<sub>2</sub> and pure H<sub>2</sub>O could be directly as feedstock for CO<sub>2</sub> overall splitting. While the APEM included special functions of the membrane electrode and electrolyte, which significantly facilitated rapid ion transfer and gas transport in the reaction. However, there are still some tough problems for MEA electrolyzers that need to be solved and improved.<sup>25,27</sup> In particular, the structure of the membrane should be further optimized to lower cell resistance, such as by altering the thickness and mechanical strength. In addition, it should be noted that the product can adhere to the surface of the membrane and even continuously cross to the anode. This is a common problem that can destroy the membrane structure, block ion transfer, and lead to degeneration of the stability. Thus, the optimization of the membrane type and structure is highly significant for further improving the device performance up to an industrial level in the future, especially regarding the stability.

### 2.5. Hybrid CO<sub>2</sub> electrolysis

The novel design strategies mentioned above mainly aim to improve the performance of the CO<sub>2</sub>RR at the cathode, including the selectivity, current density, and CO<sub>2</sub> conversion efficiency. It should be pointed out that the total the energy conversion efficiency of the CO<sub>2</sub>RR system should also be considered, which concerns the energy consumption, economic viability of the reaction system, and the net reduction of CO<sub>2</sub>.<sup>26,29,127</sup> Generally, the CO<sub>2</sub>RR is coupled with OER at the anode, which has a highly theoretical onset potential (1.23 V) and is still relatively low in terms of its efficiency of energy utilization.<sup>27,128</sup> Also, this OER process will consume 90% of the electric energy in the CO<sub>2</sub>RR system.<sup>28</sup> It is thus necessary and applicable to replace the OER at the anode by a valuable anode oxidation with a low onset potential. Within this scenario, the maximum energy conversion efficiency of the whole reaction system could be realized, such as a low cell voltage and the production of valuable chemical

products at both the anode and cathode. Therefore, hybrid CO<sub>2</sub> electrolysis has aroused much attention from researchers, such as the CO<sub>2</sub>RR/H<sub>2</sub>S oxidation reaction and CO<sub>2</sub>RR/glycerol oxidation reaction (GOR).

Li *et al.* tried to couple the CO<sub>2</sub>RR with the H<sub>2</sub>S oxidation reaction in the presence of redox couples.<sup>129</sup> By using ZnO@graphene and graphene as catalysts in the cathode and anode, respectively, the CO<sub>2</sub> molecule could be efficiently converted to CO and simultaneously H<sub>2</sub>S being a toxic and harmful gas could be oxidized to value-added products of S. Therefore, the reaction system produced win-win effects, finally achieving pollutant disposal. Moreover, there are some available and promising anode reactions with a low onset potential that can be used for nitrogen-containing wastewater treatment and chemicals synthesis to replace the OER, such as the hydrazine oxidation reaction (HzOR),<sup>130</sup> urea oxidation reaction (UOR),<sup>131,132</sup> and methane oxidation reaction (MOR).<sup>6,133,134</sup> If they are coupled with the CO<sub>2</sub>RR, it would enable the development of a reaction system with high economic and environmental benefits driven by a low cell voltage, as schematically shown in Fig. 7.

In addition, based on the thermodynamic potential and the economic feasibility of the CO<sub>2</sub>RR system, Kenis *et al.* systematically evaluated several anodic reactions that could be coupled with the CO<sub>2</sub>RR.<sup>28</sup> As a result, it was found that GOR could be used for producing biodiesel (glycerol: industrial waste) with a low onset potential, as shown in Fig. 7, and be much promising anodic reaction for marrying with the CO<sub>2</sub>RR. Using Pt/C as the catalyst for GOR, it was demonstrated that the cell voltage could be significantly reduced in comparison to that of the coupled oxygen evolution at the anode. Furthermore, by using Cu as a catalyst for the CO<sub>2</sub>RR, similar effects on the cell voltage for the electroreduction of CO<sub>2</sub> to HCOO<sup>-</sup>, C<sub>2</sub>H<sub>4</sub>, and C<sub>2</sub>H<sub>5</sub>OH were also presented, respectively. Compared with the conventional CO<sub>2</sub>RR system, this hybrid reaction system allowed saving 53% of the electricity requirements. In view of this, rationally coupling the CO<sub>2</sub>RR process with oxidation reactions to make value-added chemicals would greatly enhance the CO<sub>2</sub> utilization potential and the economic viability.

In addition, with the growing development of the organic electrooxidation reactions, some significant organic molecule oxidation reactions that can produce value-added fine chemicals should also be considered for coupling with the CO<sub>2</sub>RR. For example, 5-hydroxymethylfurfural (HMF) can be electrooxidized to 2,5-furandicarboxylic acid (FDCA), which is a significant

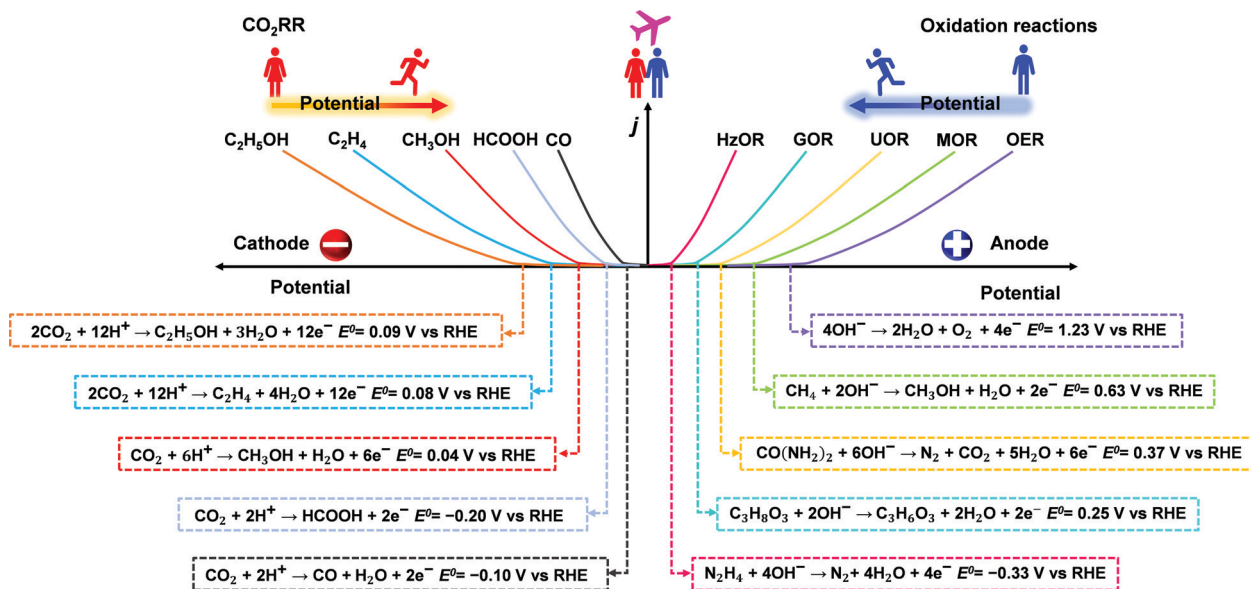


Fig. 7 Schematic diagram of polarization curves for the CO<sub>2</sub>RR and other available/potential oxidation reactions with a low onset potential, such as HzOR, GOR, UOR, and MOR. Coupling CO<sub>2</sub>RR with valuable oxidation reactions can realize high energy efficiency toward producing the target products at both the anode and cathode.

monomer for producing important polymeric materials. In addition, 3-hydroxy decanoic acid (3-HDA), derived from glucose or xylose waste-streams, can be converted into a drop-in oxygenate diesel fuel *via* an electrooxidation reaction.<sup>135</sup> Certainly, there are also more available organic oxidation reactions to replace OER, which can take inspiration from the hybrid electrolysis of water in the previous literature.<sup>136,137</sup> To make the optimal choice, relevant assessments regarding the economy, technology, and CO<sub>2</sub> net emissions among these alternative organic oxidation reactions are highly required.

### 3. Conclusions and outlook

In this account, we concentrated on the innovative design strategies for the CO<sub>2</sub>RR system, and systematically considered the various challenges for each component of the CO<sub>2</sub>RR system. In this booming field, the novel ideas emerging in retrospective work all add to facilitating the practical application of the CO<sub>2</sub>RR. It is particularly highlighted that the development and optimization of GDE or 3D free-standing electrodes, membranes, and catalysts are the key points to achieve the industrial level application in the future and require special attention. However, in some specific aspects, there are also many opportunities for researchers to further develop and explore, and tough challenges to be addressed, including the following:

(1) Multifunctional tandem catalysts by using a carbon-based catalyst (single atom) as support for target products, especially Cu-based catalysts integrated on them, will greatly attract the attention of researchers to further investigate them in terms of their mechanism and performance improvement possible. Of course, some electrocatalysts (Sn, In, Bi, Pd, Zn, and alloys, *etc.*) that can produce liquid phase products, such as

formic acid and methanol,<sup>138–143</sup> should also be considered as one of the main components of the tandem catalyst. Meanwhile, improving the stability of tandem catalysts with multiple components is a great challenge. Also, the reaction process is more uncertain, involving the adsorption and conversion of various intermediates, multi-phase interface, *etc.* Various *in situ* techniques, such as surface-enhanced Raman spectroscopy, surface-enhanced infrared absorption spectroscopy, X-ray absorption spectroscopy, need to be developed and adopted to decouple the complex reaction process.<sup>144</sup> Besides, on-chip electrocatalytic microdevice of the CO<sub>2</sub>RR should also be constructed by means of individual nanowires/nanosheets as model catalyst for directly probing electrochemical processes, monitoring dynamic changes of the catalyst, and identifying the real active sites at the nanoscale, which will greatly facilitate gaining a deeper understanding of the catalytic mechanism and will further guide the design and synthesis of the tandem catalyst.<sup>145</sup>

(2) The use of seawater as an abundant and economical electrolyte has many unique advantages. Given the complex composition of seawater, the development of various electrocatalysts that can be operated in seawater to generate value-added fuels will become a new research hotspot. Since seawater can dissolve CO<sub>2</sub> by itself, it should be a promising electrolyte for achieving a net reduction of CO<sub>2</sub>.<sup>98</sup> As for seawater electrolyte systems, there also remains some challenges, such as microbial contamination and the adsorption of complex cations and anions (Mg<sup>2+</sup>, Ca<sup>2+</sup>, Br<sup>-</sup>, I<sup>-</sup>, Cl<sup>-</sup>) on the surface of the electrode. In future, more effort should be devoted to overcome these challenges *via* coupling with mature/industrial seawater treatment techniques, such as multistage distillation and reverse osmosis, as well as the novel seawater-related techniques, such as the membrane separation process or

advanced capacitive deionization technique, to remove impurity ions.<sup>146–148</sup> The appropriate operating conditions, such as pH value, temperature, and concentration of electrolyte, should also be optimized.<sup>149–151</sup> Besides, although the solid electrolyte system has been attempted to produce pure products, more solid electrolyte systems are expected to be developed inspired by the solid-state ion batteries developed for the CO<sub>2</sub>RR.

(3) The 3D free-standing electrode structure is also popular in modularized flow-cell devices, especially 3D free-standing gas diffusion membrane electrodes. In particular, membrane electrodes, with a function of CO<sub>2</sub> capture and separation, may represent a promising research direction that needs to be focused on.<sup>152,153</sup> In this case, the exhaust gases (e.g. industrial flue gas) can be directly reutilized as feedstocks for CO<sub>2</sub>RR. In addition, the mechanical properties of the 3D free-standing electrode should be enhanced to meet the special conditions, such as high gas pressure and fast flow rate. Meanwhile, the mass transfer channels on the 3D free-standing electrode should also be well-designed and optimized at the nanoscale by using advanced 3D printing technology to increase the mass transfer rate and achieve the commercial-level current density. Much work should be done to achieve these goals in the future.

(4) The engineering of the device/electrolyzer should also be paid more attention in order to meet the practical targets related to the industrial current density and actual CO<sub>2</sub> conversion efficiency. Besides, the membrane, as the key module in MEA and APEM devices, still presents great challenges related to the stability, due to the detrimental process from products crossing and the ion shuttle. Thus, a stable membrane that can inhibit products crossing and be much more selective in passing ions is highly required.<sup>27</sup> Meanwhile, the models regarding to the fluid flow in the electrolyzer and the electrical double layer (EDL) on electrode also urgently need to be perfected/developed to guide the design of the electrolyzer.<sup>154</sup>

(5) For hybrid CO<sub>2</sub> electrolysis, the anodic reaction should be considered and analyzed from an energy-effective and economical perspective, while the electrochemical oxidation reaction for waste water treatment and fine chemicals synthesis may be taken into consideration to replace the OER at the anode. The oxidation reactions for some organic molecules are also very promising, such as 5-hydroxymethylfurfural (HMF),<sup>155</sup> benzyl alcohol (BA)<sup>156</sup> and 3-hydroxy decanoic acid (3-HDA).<sup>135</sup> Nevertheless, highly active catalysts are still urgently needed for improving the activity and selectivity. Also, oxidation reactions related to the value-added fine chemicals and the corresponding separation process still need to be developed. Once the separation techniques in the traditional chemical industry are well coupled with the CO<sub>2</sub>RR, hybrid CO<sub>2</sub> electrolysis driven by the sustainable, intermittent, and green energy will be meaningful and will roundly facilitate the industrial development of CO<sub>2</sub> utilization.

This review aimed to give systematic guidance to inspire more researchers to develop innovative design strategies for CO<sub>2</sub>RR system. Ultimately, keeping innovative strategies in mind, it is expected that the performance and superiorities of the CO<sub>2</sub>RR system will find comprehensive improvement,

including achieving an industrial-grade current density, high energy efficiency, and appreciable CO<sub>2</sub> conversion efficiency in the future.

## Conflicts of interest

There are no conflicts to declare.

## Acknowledgements

This work was partly supported by the National Natural Science Foundation of China (NSFC, No. 51872035), Talent Program of Rejuvenation of the Liaoning (No. XLYC1807002), the Fundamental Research Funds for the Central Universities (DUT19LAB20) and the National Key Research Development Program of China (2016YFB0101201).

## References

- Z. W. Seh, J. Kibsgaard, C. F. Dickens, I. Chorkendorff, J. K. Nørskov and T. F. Jaramillo, *Science*, 2017, **355**, eaad4998.
- L. Fan, C. Xia, F. Yang, J. Wang, H. Wang and Y. Lu, *Sci. Adv.*, 2020, **6**, eaay3111.
- Y. Y. Birdja, E. Pérez-Gallent, M. C. Figueiredo, A. J. Göttle, F. Calle-Vallejo and M. T. M. Koper, *Nat. Energy*, 2019, **4**, 732–745.
- P. De Luna, C. Hahn, D. Higgins, S. A. Jaffer, T. F. Jaramillo and E. H. Sargent, *Science*, 2019, **364**, eaav3506.
- T. Burdyny and W. A. Smith, *Energy Environ. Sci.*, 2019, **12**, 1442–1453.
- A. J. Martín and J. Pérez-Ramírez, *Joule*, 2019, **3**, 2602–2621.
- W. A. Smith, T. Burdyny, D. A. Vermaas and H. Geerlings, *Joule*, 2019, **3**, 1822–1834.
- R. A. Tufa, D. Chanda, M. Ma, D. Aili, T. B. Demissie, J. Vaes, Q. Li, S. Liu and D. Pant, *Appl. Energy*, 2020, **277**, 115557.
- T. Moeller, W. Ju, A. Bagger, X. Wang, F. Luo, T. N. Thanh, A. Varela, J. Rossmeisl and P. Strasser, *Energy Environ. Sci.*, 2019, **12**, 640–647.
- T. Zheng, K. Jiang, N. Ta, Y. Hu, J. Zeng, J. Liu and H. Wang, *Joule*, 2018, **3**, 265–278.
- H.-Y. Jeong, M. Balamurugan, V. S. K. Choutipalli, E.-s. Jeong, V. Subramanian, U. Sim and K. T. Nam, *J. Mater. Chem. A*, 2019, **7**, 10651–10661.
- K. Jiang, S. Siahrostami, T. Zheng, Y. Hu, S. Hwang, E. Stavitski, Y. Peng, J. Dynes, M. Gangisetty, D. Su, K. Attenkofer and H. Wang, *Energy Environ. Sci.*, 2018, **11**, 893–903.
- D. Gao, R. M. Arán-Ais, H. S. Jeon and B. Roldan Cuenya, *Nat. Catal.*, 2019, **2**, 198–210.
- G. M. Tomboc, S. Choi, T. Kwon, Y. J. Hwang and K. Lee, *Adv. Mater.*, 2020, **32**, 1908398.
- S. Nitopi, E. Bertheussen, S. B. Scott, X. Liu, A. K. Engstfeld, S. Horch, B. Seger, I. E. L. Stephens, K. Chan, C. Hahn,



- J. K. Nørskov, T. F. Jaramillo and I. Chorkendorff, *Chem. Rev.*, 2019, **119**, 7610–7672.
- 16 Y. Wang, Z. Wang, C.-T. Dinh, J. Li, A. Ozden, M. Golam Kibria, A. Seifitokaldani, C.-S. Tan, C. M. Gabardo, M. Luo, H. Zhou, F. Li, Y. Lum, C. McCallum, Y. Xu, M. Liu, A. Proppe, A. Johnston, P. Todorovic, T.-T. Zhuang, D. Sinton, S. O. Kelley and E. H. Sargent, *Nat. Catal.*, 2019, **3**, 98–106.
- 17 S. Y. Lee, S. Y. Chae, H. Jung, C. W. Lee, D. L. T. Nguyen, H.-S. Oh, B. K. Min and Y. J. Hwang, *J. Mater. Chem. A*, 2020, **8**, 6210–6218.
- 18 Y. Zheng, A. Vasileff, X. Zhou, Y. Jiao, M. Jaroniec and S.-Z. Qiao, *J. Am. Chem. Soc.*, 2019, **141**, 7646–7659.
- 19 M. B. Ross, P. De Luna, Y. Li, C.-T. Dinh, D. Kim, P. Yang and E. H. Sargent, *Nat. Catal.*, 2019, **2**, 648–658.
- 20 H. Yang, X. Wang, Q. Hu, X. Chai, X. Ren, Q. Zhang, J. Liu and C. He, *Small Methods*, 2020, **4**, 1900826.
- 21 J. Zhang, W. Luo and A. Züttel, *J. Mater. Chem. A*, 2019, **7**, 26285–26292.
- 22 J. B. Greenblatt, D. J. Miller, J. W. Ager, F. A. Houle and I. D. Sharp, *Joule*, 2018, **2**, 381–420.
- 23 Z. Sun, T. Ma, H. Tao, Q. Fan and B. Han, *Chem*, 2017, **3**, 560–587.
- 24 M. G. Kibria, J. P. Edwards, C. M. Gabardo, C.-T. Dinh, A. Seifitokaldani, D. Sinton and E. H. Sargent, *Adv. Mater.*, 2019, **31**, 1807166.
- 25 S. Hernandez-Aldave and E. Andreoli, *Catalysts*, 2020, **10**, 713.
- 26 J. Na, B. Seo, J. Kim, C. W. Lee, H. Lee, Y. J. Hwang, B. K. Min, D. K. Lee, H.-S. Oh and U. Lee, *Nat. Commun.*, 2019, **10**, 5193.
- 27 O. G. Sánchez, Y. Y. Birdja, M. Bulut, J. Vaes, T. Breugelmans and D. Pant, *Curr. Opin. Green Sustainable Chem.*, 2019, **16**, 47–56.
- 28 S. Verma, S. Lu and P. J. A. Kenis, *Nat. Energy*, 2019, **4**, 466–474.
- 29 R. G. Grim, Z. Huang, M. T. Guarnieri, J. R. Ferrell, L. Tao and J. A. Schaidle, *Energy Environ. Sci.*, 2020, **13**, 472–494.
- 30 M. Wang, K. Torbensen, D. Salvatore, S. Ren, D. Joulié, F. Dumoulin, D. Mendoza, B. Lassalle-Kaiser, U. Işci, C. P. Berlinguette and M. Robert, *Nat. Commun.*, 2019, **10**, 3602.
- 31 X. Zhang, Z. Wu, X. Zhang, L. Li, Y. Li, H. Xu, X. Li, X. Yu, Z. Zhang, Y. Liang and H. Wang, *Nat. Commun.*, 2017, **8**, 14675.
- 32 P. T. Smith, B. Punja Benke, Z. Cao, Y. Kim, E. M. Nichols, K. Kim and C. J. Chang, *Angew. Chem., Int. Ed.*, 2018, **57**, 9684–9688.
- 33 L. Sun, V. Reddu, A. C. Fisher and X. Wang, *Energy Environ. Sci.*, 2020, **13**, 374–403.
- 34 J. Choi, P. Wagner, S. Gambhir, R. Jalili, D. R. MacFarlane, G. G. Wallace and D. L. Officer, *ACS Energy Lett.*, 2019, **4**, 666–672.
- 35 J. Choi, P. Wagner, R. Jalili, J. Kim, D. R. MacFarlane, G. G. Wallace and D. L. Officer, *Adv. Energy Mater.*, 2018, **8**, 1801280.
- 36 M. Zhu, J. Chen, L. Huang, R. Ye, J. Xu and Y.-F. Han, *Angew. Chem., Int. Ed.*, 2019, **58**, 6595–6599.
- 37 Y. Liu and C. C. L. McCrory, *Nat. Commun.*, 2019, **10**, 1683.
- 38 M. Zhu, R. Ye, K. Jin, N. Lazouski and K. Manthiram, *ACS Energy Lett.*, 2018, **3**, 1381–1386.
- 39 N. Han, Y. Wang, L. Ma, J. Wen, J. Li, H. Zheng, K. Nie, X. Wang, F. Zhao, Y. Li, J. Fan, J. Zhong, T. Wu, D. J. Miller, J. Lu, S.-T. Lee and Y. Li, *Chem*, 2017, **3**, 652–664.
- 40 H. B. Yang, S.-F. Hung, S. Liu, K. Yuan, S. Miao, L. Zhang, X. Huang, H.-Y. Wang, W. Cai, R. Chen, J. Gao, X. Yang, W. Chen, Y. Huang, H. M. Chen, C. M. Li, T. Zhang and B. Liu, *Nat. Energy*, 2018, **3**, 140–147.
- 41 T. Zheng, K. Jiang, N. Ta, Y. Hu, J. Zeng, J. Liu and H. Wang, *Joule*, 2019, **3**, 265–278.
- 42 C. Yan, H. Li, Y. Ye, H. Wu, F. Cai, R. Si, J. Xiao, S. Miao, S. Xie, F. Yang, Y. Li, G. Wang and X. Bao, *Energy Environ. Sci.*, 2018, **11**, 1204–1210.
- 43 K. Zhao, X. Nie, H. Wang, S. Chen, X. Quan, H. Yu, W. Choi, G. Zhang, B. Kim and J. G. Chen, *Nat. Commun.*, 2020, **11**, 2455.
- 44 J. Gu, C.-S. Hsu, L. Bai, H. M. Chen and X. Hu, *Science*, 2019, **364**, 1091–1094.
- 45 W. Ju, A. Bagger, G. P. Hao, A. S. Varela, I. Sinev, V. Bon, B. Roldan Cuenya, S. Kaskel, J. Rossmeisl and P. Strasser, *Nat. Commun.*, 2017, **8**, 944.
- 46 Y. Pan, R. Lin, Y. Chen, S. Liu, W. Zhu, X. Cao, W. Chen, K. Wu, W.-C. Cheong, Y. Wang, L. Zheng, J. Luo, Y. Lin, Y. Liu, C. Liu, J. Li, Q. Lu, X. Chen, D. Wang, Q. Peng, C. Chen and Y. Li, *J. Am. Chem. Soc.*, 2018, **140**, 4218–4221.
- 47 X. Zu, X. Li, W. Liu, Y. Sun, J. Xu, T. Yao, W. Yan, S. Gao, C. Wang, S. Wei and Y. Xie, *Adv. Mater.*, 2019, **31**, 1808135.
- 48 X. Sun, C. Chen, S. Liu, S. Hong, Q. Zhu, Q. Qian, B. Han, J. Zhang and L. Zheng, *Angew. Chem., Int. Ed.*, 2019, **58**, 4669–4673.
- 49 W. Zheng, F. Chen, Q. Zeng, Z. Li, B. Yang, L. Lei, Q. Zhang, F. He, X. Wu and Y. Hou, *Nano-Micro Lett.*, 2020, **12**, 108.
- 50 Y. Chen, C. W. Li and M. W. Kanan, *J. Am. Chem. Soc.*, 2012, **134**, 19969–19972.
- 51 C. Rogers, W. S. Perkins, G. Veber, T. E. Williams, R. R. Cloke and F. R. Fischer, *J. Am. Chem. Soc.*, 2017, **139**, 4052–4061.
- 52 S. C. Abeyweera, J. Yu, J. P. Perdew, Q. Yan and Y. Sun, *Nano Lett.*, 2020, **20**, 2806–2811.
- 53 W. Zhu, S. Kattel, F. Jiao and J. G. Chen, *Adv. Energy Mater.*, 2019, **9**, 1802840.
- 54 D. Gao, H. Zhou, F. Cai, J. Wang, G. Wang and X. Bao, *ACS Catal.*, 2018, **8**, 1510–1519.
- 55 R. Shi, J. Guo, X. Zhang, G. I. N. Waterhouse, Z. Han, Y. Zhao, L. Shang, C. Zhou, L. Jiang and T. Zhang, *Nat. Commun.*, 2020, **11**, 3028.
- 56 N. Todoroki, H. Tei, H. Tsurumaki, T. Miyakawa, T. Inoue and T. Wadayama, *ACS Catal.*, 2019, **9**, 1383–1388.
- 57 E. L. Clark, S. Ringe, M. Tang, A. Walton, C. Hahn, T. F. Jaramillo, K. Chan and A. T. Bell, *ACS Catal.*, 2019, **9**, 4006–4014.
- 58 L. Wei, H. Li, J. Chen, Z. Yuan, Q. Huang, X. Liao, G. Henkelman and Y. Chen, *ACS Catal.*, 2020, **10**, 1444–1453.

- 59 M. Ma, K. Liu, J. Shen, R. Kas and W. A. Smith, *ACS Energy Lett.*, 2018, **3**, 1301–1306.
- 60 T.-T. Zhuang, Z.-Q. Liang, A. Seifitokaldani, Y. Li, P. De Luna, T. Burdyny, F. Che, F. Meng, Y. Min, R. Quintero-Bermudez, C. T. Dinh, Y. Pang, M. Zhong, B. Zhang, J. Li, P.-N. Chen, X.-L. Zheng, H. Liang, W.-N. Ge, B.-J. Ye, D. Sinton, S.-H. Yu and E. H. Sargent, *Nat. Catal.*, 2018, **1**, 421–428.
- 61 P. De Luna, R. Quintero-Bermudez, C.-T. Dinh, M. B. Ross, O. S. Bushuyev, P. Todorović, T. Regier, S. O. Kelley, P. Yang and E. H. Sargent, *Nat. Catal.*, 2018, **1**, 103–110.
- 62 X. Wang, Z. Wang, F. P. García de Arquer, C.-T. Dinh, A. Ozden, Y. C. Li, D.-H. Nam, J. Li, Y.-S. Liu, J. Wicks, Z. Chen, M. Chi, B. Chen, Y. Wang, J. Tam, J. Y. Howe, A. Proppe, P. Todorović, F. Li, T.-T. Zhuang, C. M. Gabardo, A. R. Kirmani, C. McCallum, S.-F. Hung, Y. Lum, M. Luo, Y. Min, A. Xu, C. P. O'Brien, B. Stephen, B. Sun, A. H. Ip, L. J. Richter, S. O. Kelley, D. Sinton and E. H. Sargent, *Nat. Energy*, 2020, **5**, 478–486.
- 63 M. Luo, Z. Wang, Y. C. Li, J. Li, F. Li, Y. Lum, D.-H. Nam, B. Chen, J. Wicks, A. Xu, T. Zhuang, W. R. Leow, X. Wang, C.-T. Dinh, Y. Wang, Y. Wang, D. Sinton and E. H. Sargent, *Nat. Commun.*, 2019, **10**, 5814.
- 64 W. Ma, S. Xie, T. Liu, Q. Fan, J. Ye, F. Sun, Z. Jiang, Q. Zhang, J. Cheng and Y. Wang, *Nat. Catal.*, 2020, **3**, 478–487.
- 65 P.-P. Yang, X.-L. Zhang, F.-Y. Gao, Y.-R. Zheng, Z.-Z. Niu, X. Yu, R. Liu, Z.-Z. Wu, S. Qin, L.-P. Chi, Y. Duan, T. Ma, X.-s. Zheng, J. Zhu, H.-J. Wang, M.-R. Gao and S.-H. Yu, *J. Am. Chem. Soc.*, 2020, **142**, 6400–6408.
- 66 R. M. Arán-Ais, F. Scholten, S. Kunze, R. Rizo and B. Roldan Cuenya, *Nat. Energy*, 2020, **5**, 317–325.
- 67 H. Wang, Y.-K. Tzeng, Y. Ji, Y. Li, J. Li, X. Zheng, A. Yang, Y. Liu, Y. Gong, L. Cai, Y. Li, X. Zhang, W. Chen, B. Liu, H. Lu, N. A. Melosh, Z.-X. Shen, K. Chan, T. Tan, S. Chu and Y. Cui, *Nat. Nanotechnol.*, 2020, **15**, 131–137.
- 68 M. Zhong, K. Tran, Y. Min, C. Wang, Z. Wang, C.-T. Dinh, P. De Luna, Z. Yu, A. S. Rasouli, P. Brodersen, S. Sun, O. Voznyy, C.-S. Tan, M. Askerka, F. Che, M. Liu, A. Seifitokaldani, Y. Pang, S.-C. Lo, A. Ip, Z. Ulissi and E. H. Sargent, *Nature*, 2020, **581**, 178–183.
- 69 H. Xiao, T. Cheng and W. A. Goddard, *J. Am. Chem. Soc.*, 2017, **139**, 130–136.
- 70 K. Jiang, R. B. Sandberg, A. J. Akey, X. Liu, D. C. Bell, J. K. Nørskov, K. Chan and H. Wang, *Nat. Catal.*, 2018, **1**, 111–119.
- 71 X. Wang, Z. Wang, T.-T. Zhuang, C.-T. Dinh, J. Li, D.-H. Nam, F. Li, C.-W. Huang, C.-S. Tan, Z. Chen, M. Chi, C. M. Gabardo, A. Seifitokaldani, P. Todorović, A. Proppe, Y. Pang, A. R. Kirmani, Y. Wang, A. H. Ip, L. J. Richter, B. Scheffel, A. Xu, S.-C. Lo, S. O. Kelley, D. Sinton and E. H. Sargent, *Nat. Commun.*, 2019, **10**, 5186.
- 72 C. G. Morales-Guio, E. R. Cave, S. A. Nitopi, J. T. Feaster, L. Wang, K. P. Kuhl, A. Jackson, N. C. Johnson, D. N. Abram, T. Hatsukade, C. Hahn and T. F. Jaramillo, *Nat. Catal.*, 2018, **1**, 764–771.
- 73 F. Li, Y. C. Li, Z. Wang, J. Li, D.-H. Nam, Y. Lum, M. Luo, X. Wang, A. Ozden, S.-F. Hung, B. Chen, Y. Wang, J. Wicks, Y. Xu, Y. Li, C. M. Gabardo, C.-T. Dinh, Y. Wang, T.-T. Zhuang, D. Sinton and E. H. Sargent, *Nat. Catal.*, 2020, **3**, 75–82.
- 74 X. Wang, J. F. de Araújo, W. Ju, A. Bagger, H. Schmies, S. Köhl, J. Rossmeisl and P. Strasser, *Nat. Nanotechnol.*, 2019, **14**, 1063–1070.
- 75 X. Wang, Q. Zhao, B. Yang, Z. Li, Z. Bo, K.-h. Lam, N. M. Adli, L. Lei, Z. Wen, G. Wu and Y. Hou, *J. Mater. Chem. A*, 2019, **7**, 25191–25202.
- 76 A. S. Varela, W. Ju, A. Bagger, P. Franco, J. Rossmeisl and P. Strasser, *ACS Catal.*, 2019, **9**, 7270–7284.
- 77 Y. Wu, Z. Jiang, X. Lu, Y. Liang and H. Wang, *Nature*, 2019, **575**, 639–642.
- 78 E. Boutin, M. Wang, J. C. Lin, M. Mesnage, D. Mendoza, B. Lassalle-Kaiser, C. Hahn, T. F. Jaramillo and M. Robert, *Angew. Chem., Int. Ed.*, 2019, **58**, 16172–16176.
- 79 A. B. Jorge, R. Jervis, A. P. Periasamy, M. Qiao, J. Feng, L. N. Tran and M.-M. Titirici, *Adv. Energy Mater.*, 2020, **10**, 2070047.
- 80 J. Liu, H. Zhang, M. Qiu, Z. Peng, M. K. H. Leung, W.-F. Lin and J. Xuan, *J. Mater. Chem. A*, 2020, **8**, 2222–2245.
- 81 Z. Chen, S. Yao and L. Liu, *J. Mater. Chem. A*, 2017, **5**, 24651–24656.
- 82 D. M. Weekes, D. A. Salvatore, A. Reyes, A. Huang and C. P. Berlinguette, *Acc. Chem. Res.*, 2018, **51**, 910–918.
- 83 D. A. Salvatore, D. M. Weekes, J. He, K. E. Dettelbach, Y. C. Li, T. E. Mallouk and C. P. Berlinguette, *ACS Energy Lett.*, 2018, **3**, 149–154.
- 84 W.-H. Cheng, M. H. Richter, I. Sullivan, D. M. Larson, C. Xiang, B. S. Brunshwig and H. A. Atwater, *ACS Energy Lett.*, 2020, **5**, 470–476.
- 85 M. Ma, E. L. Clark, S. Dalsgaard, K. T. Therkildsen, I. Chorkendorff and B. J. Seger, *Energy Environ. Sci.*, 2020, **13**, 977–985.
- 86 F. P. García de Arquer, C.-T. Dinh, A. Ozden, J. Wicks, C. McCallum, A. R. Kirmani, D.-H. Nam, C. Gabardo, A. Seifitokaldani, X. Wang, Y. C. Li, F. Li, J. Edwards, L. J. Richter, S. J. Thorpe, D. Sinton and E. H. Sargent, *Science*, 2020, **367**, 661–666.
- 87 V. Vedharathinam, Z. Qi, C. Horwood, B. Bourcier, M. Stadermann, J. Biener and M. Biener, *ACS Catal.*, 2019, **9**, 10605–10611.
- 88 H. Yang, Q. Lin, C. Zhang, X. Yu, Z. Cheng, G. Li, Q. Hu, X. Ren, Q. Zhang, J. Liu and C. He, *Nat. Commun.*, 2020, **11**, 593.
- 89 C. Chen, X. Sun, X. Yan, Y. Wu, H. Liu, Q. Zhu, B. B. A. Bediako and B. Han, *Angew. Chem., Int. Ed.*, 2020, **59**, 11123–11129.
- 90 D. Gao, I. Sinev, F. Scholten, R. M. Arán-Ais, N. J. Divins, K. Kvashnina, J. Timoshenko and B. Roldán Cuenya, *Angew. Chem., Int. Ed.*, 2019, **58**, 17047–17053.
- 91 T. Li, C. Yang, J.-L. Luo and G. Zheng, *ACS Catal.*, 2019, **9**, 10440–10447.
- 92 M. Moura de Salles Pupo and R. Kortlever, *ChemPhysChem*, 2019, **20**, 2926–2935.

- 93 J. Resasco, L. D. Chen, E. Clark, C. Tsai, C. Hahn, T. F. Jaramillo, K. Chan and A. T. Bell, *J. Am. Chem. Soc.*, 2017, **139**, 11277–11287.
- 94 R. M. Arán-Ais, D. Gao and B. Roldan Cuenya, *Acc. Chem. Res.*, 2018, **51**, 2906–2917.
- 95 J.-J. Lv, M. Jouny, W. Luc, W. Zhu, J.-J. Zhu and F. Jiao, *Adv. Mater.*, 2018, **30**, 1803111.
- 96 S. Verma, X. Lu, S. Ma, R. I. Masel and P. J. A. Kenis, *Phys. Chem. Chem. Phys.*, 2016, **18**, 7075–7084.
- 97 M. König, J. Vaes, E. Klemm and D. Pant, *iScience*, 2019, **19**, 135–160.
- 98 A. Chen and B.-L. Lin, *Joule*, 2018, **2**, 594–606.
- 99 B. A. Rosen, A. Salehi-Khojin, M. R. Thorson, W. Zhu, D. T. Whipple, P. J. A. Kenis and R. I. Masel, *Science*, 2011, **334**, 643–644.
- 100 M. Asadi, K. Kim, C. Liu, A. V. Addepalli, P. Abbasi, P. Yasaei, P. Phillips, A. Behranginia, J. M. Cerrato, R. Haasch, P. Zapol, B. Kumar, R. F. Klie, J. Abiade, L. A. Curtiss and A. Salehi-Khojin, *Science*, 2016, **353**, 467–470.
- 101 C. T. Dinh, T. Burdyny, M. G. Kibria, A. Seifitokaldani, C. M. Gabardo, F. P. Garcia de Arquer, A. Kiani, J. P. Edwards, P. De Luna, O. S. Bushuyev, C. Zou, R. Quintero-Bermudez, Y. Pang, D. Sinton and E. H. Sargent, *Science*, 2018, **360**, 783–787.
- 102 J. Zhang, W. Luo and A. Züttel, *J. Catal.*, 2020, **385**, 140–145.
- 103 F. Quan, D. Zhong, H. Song, F. Jia and L. Zhang, *J. Mater. Chem. A*, 2015, **3**, 16409–16413.
- 104 D. Gao, I. T. McCrum, S. Deo, Y.-W. Choi, F. Scholten, W. Wan, J. G. Chen, M. J. Janik and B. Roldan Cuenya, *ACS Catal.*, 2018, **8**, 10012–10020.
- 105 D. Gao, F. Scholten and B. Roldan Cuenya, *ACS Catal.*, 2017, **7**, 5112–5120.
- 106 A. S. Varela, W. Ju, T. Reier and P. Strasser, *ACS Catal.*, 2016, **6**, 2136–2144.
- 107 F. Quan, G. Zhan, H. Shang, Y. Huang, F. Jia, L. Zhang and Z. Ai, *Green Chem.*, 2019, **21**, 3256–3262.
- 108 A. S. Varela, W. Ju and P. Strasser, *Adv. Energy Mater.*, 2018, **8**, 1703614.
- 109 J. Li, D. Wu, A. S. Malkani, X. Chang, M.-J. Cheng, B. Xu and Q. Lu, *Angew. Chem., Int. Ed.*, 2019, **11**, 4464–4469.
- 110 K. Nakata, T. Ozaki, C. Terashima, A. Fujishima and Y. Einaga, *Angew. Chem., Int. Ed.*, 2014, **53**, 871–874.
- 111 C.-Y. Lee and G. G. Wallace, *J. Mater. Chem. A*, 2018, **6**, 23301–23307.
- 112 D. Qu, X. Peng, Y. Mi, H. Bao, S. Zhao, X. Liu and J. Luo, *Nanoscale*, 2020, **12**, 17191–17195.
- 113 Q. Wu, J. Gao, J. Feng, Q. Liu, Y. Zhou, S. Zhang, M. Nie, Y. Liu, J. Zhao, F. Liu, J. Zhong and Z. Kang, *J. Mater. Chem. A*, 2020, **8**, 1205–1211.
- 114 H. D. Willauer, F. DiMascio, D. R. Hardy and F. W. Williams, *Ind. Eng. Chem. Res.*, 2014, **53**, 12192–12200.
- 115 S. Dresp, F. Dionigi, M. Klingenhof and P. Strasser, *ACS Energy Lett.*, 2019, **4**, 933–942.
- 116 Y. Kuang, M. J. Kenney, Y. Meng, W. H. Hung, Y. Liu, J. E. Huang, R. Prasanna, P. Li, Y. Li, L. Wang, M. C. Lin, M. D. McGehee, X. Sun and H. Dai, *Proc. Natl. Acad. Sci. U. S. A.*, 2019, **116**, 6624–6629.
- 117 D. D. Zhu, J. L. Liu and S. Z. Qiao, *Adv. Mater.*, 2016, **28**, 3423–3452.
- 118 Q. Dong, X. Zhang, D. He, C. Lang and D. Wang, *ACS Cent. Sci.*, 2019, **5**, 1461–1467.
- 119 C. Xia, P. Zhu, Q. Jiang, Y. Pan, W. Liang, E. Stavitsk, H. N. Alshareef and H. Wang, *Nat. Energy*, 2019, **4**, 776–785.
- 120 F.-Y. Gao, R.-C. Bao, M.-R. Gao and S.-H. Yu, *J. Mater. Chem. A*, 2020, **8**, 15458–15478.
- 121 G. M. Sriramagiri, N. Ahmed, W. Luc, K. D. Dobson, S. S. Hegedus and F. Jiao, *ACS Sustainable Chem. Eng.*, 2017, **5**, 10959–10966.
- 122 T. Li, E. W. Lees, M. Goldman, D. A. Salvatore, D. M. Weekes and C. P. Berlinguette, *Joule*, 2019, **3**, 1487–1497.
- 123 C. M. Gabardo, C. P. O'Brien, J. P. Edwards, C. McCallum, Y. Xu, C.-T. Dinh, J. Li, E. H. Sargent and D. Sinton, *Joule*, 2019, **3**, 2777–2791.
- 124 D. S. Ripatti, T. R. Veltman and M. W. Kanan, *Joule*, 2019, **3**, 240–256.
- 125 B. Endrődi, E. Kecsenovity, A. Samu, F. Darvas, R. V. Jones, V. Török, A. Danyi and C. Janáky, *ACS Energy Lett.*, 2019, **4**, 1770–1777.
- 126 Z. Yin, H. Peng, X. Wei, H. Zhou, J. Gong, M. Huai, L. Xiao, G. Wang, J. Lu and L. Zhuang, *Energy Environ. Sci.*, 2019, **12**, 2455–2462.
- 127 B. M. Tackett, E. Gomez and J. G. Chen, *Nat. Catal.*, 2019, **2**, 381–386.
- 128 B. You and Y. Sun, *Acc. Chem. Res.*, 2018, **51**, 1571–1580.
- 129 W. Ma, H. Wang, W. Yu, X. Wang, Z. Xu, X. Zong and C. Li, *Angew. Chem., Int. Ed.*, 2018, **57**, 3473–3477.
- 130 J. Y. Zhang, H. Wang, Y. Tian, Y. Yan, Q. Xue, T. He, H. Liu, C. Wang, Y. Chen and B. Y. Xia, *Angew. Chem., Int. Ed.*, 2018, **57**, 7649–7653.
- 131 Z.-Y. Yu, C.-C. Lang, M.-R. Gao, Y. Chen, Q.-Q. Fu, Y. Duan and S.-H. Yu, *Energy Environ. Sci.*, 2018, **11**, 1890–1897.
- 132 L. Zhang, L. Wang, H. Lin, Y. Liu, J. Ye, Y. Wen, A. Chen, L. Wang, F. Ni, Z. Zhou, S. Sun, Y. Li, B. Zhang and H. Peng, *Angew. Chem., Int. Ed.*, 2019, **58**, 16820–16825.
- 133 H. Yin, Y. Dou, S. Chen, Z. Zhu, P. Liu and H. Zhao, *Adv. Mater.*, 2019, **32**, 1904870.
- 134 M. Ma, C. Oh, J. Kim, J. H. Moon and J. H. Park, *Appl. Catal., B*, 2019, **259**, 118095.
- 135 J. Meyers, J. B. Mensah, F. J. Holzhäuser, A. Omari, C. C. Blesken, T. Tiso, S. Palkovits, L. M. Blank, S. Pischinger and R. Palkovits, *Energy Environ. Sci.*, 2019, **12**, 2406–2411.
- 136 Y. Xu and B. Zhang, *ChemElectroChem*, 2019, **6**, 3214–3226.
- 137 B. You and Y. Sun, *Acc. Chem. Res.*, 2018, **51**, 1571–1580.
- 138 W. Zhang, Q. Qin, L. Dai, R. Qin, X. Zhao, X. Chen, D. Ou, J. Chen, T. T. Chuong, B. Wu and N. Zheng, *Angew. Chem., Int. Ed.*, 2018, **57**, 9475–9479.

- 139 D. Yang, Q. Zhu, C. Chen, H. Liu, Z. Liu, Z. Zhao, X. Zhang, S. Liu and B. Han, *Nat. Commun.*, 2019, **10**, 677.
- 140 F. Yang, A. O. Elnabawy, R. Schimmenti, P. Song, J. Wang, Z. Peng, S. Yao, R. Deng, S. Song, Y. Lin, M. Mavrikakis and W. Xu, *Nat. Commun.*, 2020, **11**, 1088.
- 141 W. Ma, S. Xie, X.-G. Zhang, F. Sun, J. Kang, Z. Jiang, Q. Zhang, D.-Y. Wu and Y. Wang, *Nat. Commun.*, 2019, **10**, 892.
- 142 W. Deng, L. Zhang, L. Li, S. Chen, C. Hu, Z.-J. Zhao, T. Wang and J. Gong, *J. Am. Chem. Soc.*, 2019, **141**, 2911–2915.
- 143 Q. H. Low, N. W. X. Loo, F. Calle-Vallejo and B. S. Yeo, *Angew. Chem., Int. Ed.*, 2019, **58**, 2256–2260.
- 144 X. Li, S. Wang, L. Li, Y. Sun and Y. Xie, *J. Am. Chem. Soc.*, 2020, **142**, 9567–9581.
- 145 H. Yang, Q. He, Y. Liu, H. Li, H. Zhang and T. Zhai, *Chem. Soc. Rev.*, 2020, **49**, 2916–2936.
- 146 T. Wu, G. Wang, Q. Dong, F. Zhan, X. Zhang, S. Li, H. Qiao and J. Qiu, *Environ. Sci. Technol.*, 2017, **51**, 9244–9251.
- 147 S. Wang, G. Wang, T. Wu, Y. Zhang, F. Zhan, Y. Wang, J. Wang, Y. Fu and J. Qiu, *J. Mater. Chem. A*, 2018, **6**, 14644–14650.
- 148 Y. Cho, K. S. Lee, S. Yang, J. Choi, H.-r. Park and D. K. Kim, *Energy Environ. Sci.*, 2017, **10**, 1746–1750.
- 149 D. Sören, D. Fabio, L. Stefan, F. d. A. Jorge, S. Camillo, G. Manuel, D. Holger and S. Peter, *Adv. Energy Mater.*, 2018, **8**, 1800338.
- 150 F. Dionigi, T. Reier, Z. Pawolek, M. Gliech and P. Strasser, *ChemSusChem*, 2016, **9**, 962–972.
- 151 W. Tong, M. Forster, F. Dionigi, S. Dresp, R. Sadeghi Erami, P. Strasser, A. J. Cowan and P. Farràs, *Nat. Energy*, 2020, **5**, 367–377.
- 152 Y. Xu, J. P. Edwards, J. Zhong, C. O'Brien, C. M. Gabardo, C. McCallum, J. Li, T. C. Dinh, E. H. Sargent and D. Sinton, *Energy Environ. Sci.*, 2020, **13**, 554–561.
- 153 P. Li, X. Lu, Z. Wu, Y. Wu, R. Malpass-Evans, N. B. McKeown, X. Sun and H. Wang, *Angew. Chem., Int. Ed.*, 2020, **59**, 1–7.
- 154 D. Bohra, J. H. Chaudhry, T. Burdyny, E. A. Pidko and W. A. Smith, *Energy Environ. Sci.*, 2019, **12**, 3380–3389.
- 155 W.-J. Liu, L. Dang, Z. Xu, H.-Q. Yu, S. Jin and G. W. Huber, *ACS Catal.*, 2018, **8**, 5533–5541.
- 156 X. Liu, N. Jiang and Y. Sun, *J. Am. Chem. Soc.*, 2016, **138**, 13639–13646.